Assessment and Characterization of Road Embankment Failure Along Bako-Shanbu Road Project

Zerihun Kuma Tesema

A Thesis Submitted to the department of civil Engineering

College of Civil engineering and architecture

Office of Postgraduate Studies

Adama Science and Technology University

June, 2025

Adama, Ethiopia

Assessment and Characterization of Road Embankment Failure Along Bako-Shanbu Road Project

Zerihun Kuma Tesema

Advisor: Biruk Gissila (PhD)

A Thesis Submitted to the department of civil Engineering

College of civil engineering and architecture

Office of Postgraduate Studies

Adama Science and Technology University

June, 2025

Adama, Ethiopia

Declaration

I declare that this thesis proposal entitled "Assessment and Characterization of Road Embankment Failure along Bako-Shanbu Road Project" is my own work and has not been submitted to any university for similar purpose. The references used in this proposal are duly recognized by proper citations.

Zerihun Kuma Tesema	___________________	________________
Name of Student	Signature	Date

Recommendation of Advisors/ Supervisors

I, the major advisor/supervisor of this research proposal, hereby certify that I ha closely advised/supervised the student while developing this proposal and read the draft thesis proposal entitled "Assessment and Characterization of Road Embankment Failure along Bako-Shanbu Road Project" prepared under my guidance by Zerihun Kuma Tesema. Therefore, I recommend the submission of the proposal to the department for further review and evaluation.

Biruk Gissila (PhD)		
Major Advisor/Supervisor	Signature	Date
Co-advisor/Co-supervisor	Signature	Date

Approval Page

I/we hereby certify that the recommendation and suggestion given by the proposal review committee are appropriately incorporated into the final thesis proposal entitled "Assessment and Characterization of Road Embankment Failure along Bako-Shanbu Road Project" by Zerihun Kuma Tesema.

Biruk Gissila (PhD)		
Major Advisor/Supervisor	Signature	Date
Co-advisor/Co-supervisor	Signature	Date

Approval of Board of Reviewers

We, the undersigned, members of the Board of Reviewers of the proposal open defense by Zerihun Kuma Tesema have read and evaluated the thesis proposal entitled "Assessment and Characterization of Road Embankment Failure along Bako-Shanbu Road Project" and assessed the understanding of the candidate about the proposed research. This is, therefore, to certify that the thesis proposal is accepted and we recommend the implementation of the proposal.

___________________________	____________________	__________________
Chairperson	Signature	Date
___________________________	____________________	__________________
Reviewer 1	Signature	Date
___________________________	____________________	__________________
Reviewer 2	Signature	Date

Finally, approval and acceptance of the thesis proposal is contingent upon submission of its final copy to the Office of Postgraduate Studies (OPGS) through the Department Graduate Council (DGC) and School Graduate Committee (SGC).

___________________________	____________________	__________________
Department Head	Signature	Date
___________________________	____________________	__________________
College Dean	Signature	Date
___________________________	____________________	__________________
Office of Postgraduate Stud	Dean Signature	Date

ACKNOWLEDGMENT

Thanks to be God almighty, the most merciful, for giving me the ability, the health, and the strength to start this work. I would like to express my deep gratitude to my Advisor, Dr.Biruk Gissela for his incredible feeding of knowledge and selecting this title. He offered me all the necessary knowledge, experience, and support required to successfully complete this Thesis. It was a great pleasure for me to have him. His help and support is really appreciated and also I want thank my friend Seid Nuru who is my senior Geotechnical Engineering student he share me his journey in thesis.

I am also thankful to Adama Science and technology University and the staff of university for their cooperation in providing the necessary information about the area in relation to my work with their great politeness, not only this but also I want to thank my family they are big source of inspirations throughout my academic career with their valuable moral supportandadvice.

Table of Contents

LIST OF TABLE

LIST OF FIGURES

List of Acronyms and Abbreviations

AASHTO………………American Association of State Highway and Transportation Officials

ASTM………………….American Society for Testing Materials

PI……………………….Plastic Index

MDD……………………Maximum Dry Density

PI………………………..Plastic Limit

LL……………………… Liquid Limit

ERA……………………..Ethiopian Roads Authority

ϕ...………………………Angle of Internal Friction

C……………… ………cohesion

γ………………… ……Unit weight

FOS…………………...…Factor Of Safety

LL………………………..Liquid Limit

PL……………………..….Plastic Limit

PI……………………...…Plastic Index

Abstract

Road embankment failure is a serious natural disaster that can cause a damage on both human and animal lives, disrupt traffic, and even cause land to slide into rivers. Recently, a significant embankment failure along the Bako-Shambu road project in the Oromia region, specifically in the western Wellega zone have been occured. This study is focused on assessing and understanding the embankment failures happening along this road. During a visual inspection, we identified that the main concern in the Bako-Shambu road project is indeed the embankment failures, which have had a notable economic impact on local communities and have led to serious accidents along the route from Bako to Shambu. To gather data, we conducted site investigations at various points along the Bako-Shambu road project, particularly at Sites 1, 3, 5, 6, 7, 9, and the seven sections where embankments have failed. Both disturbed and undisturbed soil samples for laboratory testing have been collected, which included Atterberg limits, moisture content, specific gravity, unit weight, soil classification, and direct shear tests to analyze soil parameters. The lab results showed that the soil is clayey and highly plastic, with a significant swelling potential and sensitivity to moisture, which can lead to sliding. The grain size analysis indicated that more than 71% of the soil consists of fine-grained materials, primarily high plastic clay that becomes unstable when wet. Furthermore, the specific gravity measurements suggest that the soil within the range for clay and silty clay, which has multiple planes of weakness that can contribute to slope instability.

The stability analysis of the slope was conducted using Geostudio/SlopW 2024 software, exploring various scenarios. The first scenario involves a fully saturated water table, which represents the worst-case situation, typically occurring during heavy rainfall or flooding. In this case, the factor of safety (FS) decreases across different methods. In the second scenario, where the water table is at the toe of the embankment, the FS value starts to increase.

Keywords: *Embankment Failure, Slope Stability, Slope Failure, Geostudio/SlopeW, embankment, Slope failure*

CHAPTER ONE

Introduction

1.1. Background

Landslides are one of the most serious environmental threats on the planet. Annually, landslides cause significant harm to a large number of private and public assets.Countries invest significant financial capital in mitigating this disruption (Che Mamat et al.2022).

On the African continent, in spite of their socio-economic impacts, landslides are only rarely studied (Maes et al., 2017) and systematic landslide hazard investigations in sub-Sahara Africa are particularly rare (e.g. Knapen et al., 2006; Van Den et al., 2009; Che et al., 2011; Maki and Dewitte, 2014) Wendim, S., Woldearegay, K., & Mebrahtu, G. (2023).

In Ethiopia, landslide-generated hazards are becoming serious concerns to the general public and to the planners and decision-makers at various levels of the government. However, so far, little efforts have been made to reduce losses from such hazards. With the on-going infrastructural development, urbanization, rural development, and with the present land management system, it is foreseeable that the frequency and magnitude of landslides and losses due to such hazards would continue to increase unless appropriate actions are taken in the Ethiopia.

The hilly and mountainous terrains of the highlands of Ethiopia which are characterized by variable topographical, geological, hydrological (surface and groundwater) and land-use conditions, are frequently affected by rainfall-triggered slope failures. Earthquake triggered landslides are little reported in Ethiopia (Kifle Weldearegay, 2013).

The current study area is located along Bako-Shambu Road in Oromia Regional State and is one of land slide area in Ethiopia. The topographic of the route corridor varies, from steep and rugged mountainous terrain to dominantly gently sloping terrain and it is vulnerable to land slide.The causes for slope failures were identified by doing field investigation, laboratory tests and slope stability analysis using Geostudio slope W software.

1.2. Statement of the Problem

In Ethiopia, hazards caused by landslides are increasingly alarming for the public as well as for planners and decision-makers across different government levels. Nevertheless, to date, minimal efforts have been undertaken to mitigate the losses associated with these hazards.

Given the current infrastructural advancements, urban expansion, rural development, and the existing land management practices, it is anticipated that the occurrence and severity of landslides, along with the resulting damages from such events, will likely rise in Ethiopia unless suitable measures are implemented. This review article has been developed to emphasize the problem of landslides and associated geohazards for the attention of academic institutions, policymakers, and pertinent organizations (Woldearegay, 2013).

The Bako-Shambu road project, situated within the West Wellega zone of Ethiopia, has encountered many failures in road embankment. The region is widely recognized for its susceptibility to landslides, attributed to its geological and geomorphic characteristics that promote slope instability. These characteristics encompass geological lithology, soil development, climatic factors, topography, and both surface and subsurface water.

The embankment failure occurred in a gently-sloping hill comprised of thick soil, which is a clay rich erodible lateritic soil. The soil is sensitive to slight moisture change is facilitating instability up on saturation during high precipitation, and groundwater rise to increase the pore pressure to sock the road layer and causes embankment and pavement failure.

The creeping and cracking pavement that caused by the spoil pilling regularly triggered by the rainfall saturation. Surface water that will seep into the soil at the head of the tension cracks. These conditions produce erosion and increase the tendency for potential surface slumps and localized failures on the slope face. associated with possible toe erosion and saturation by the nearly river found in RHS about 80m showing progressive eroding the toe and gets closer to road with time.

Consequently, the Bako-Shambu road project is confronted with significant embankment failures. These failures endanger the road's operational functionality and safety, impose substantial economic burdens, and set back the local development.

1.3. Research Questions

- What are the causes of the embankment failures observed in the study area?
- What specific soil types are present within the study area?
- In what manner can the embankment failures be accurately characterized?

1.4. Objectives of the Study

1.4.1. General Objectives

The main Objective of this study is to assess and characterize the road embankment failures occurring along the Bako-Shambu road project, particularly in between (km 94+120 to km 107+480) and Stability analysis of Site 7 at 104+140 using Geostudio/slop w software.

1.4.2. Specific Objectives

- To identify causes of the embankment failures in the study area.
- To identify the types of soil present within the study area.
- To systematically characterize the nature of the embankment failures.

1.5. Significance of the Study

The outcomes of this research concerning the Bako-Shambu road project are intended to:

- Enhance the understanding the causes of road embankment failures and their potential remedial measures.
- Facilitate improvements in the safety and quality of the road infrastructure along the Bako-Shambu project.
- To ensure the slope stability of Road Embankment failed section particularly Site 7 of the study area at a station 104+140 using Geostudio slope w software.

1.6. Scope and Limitation

The Scope of this research is to assess and characterize the road embankment failures occurring along the Bako-Shambu road project, particularly in between (km 94+120 to km 107+480).

The study consists of: (a) field investigation: during site visiting, the factors contributing to the embankment failures, stability conditions of those sections (Site 1,3,5,6,7,9, and 11) are investigated, (b) Sample collection: both Disturbed and un disturbed samples are collected from the failed embankment section in order to test, (c) laboratory testing: these tests have been carried out (Atterberg limit, Grain size analysis, specific gravity and unit weight) for the assessment of index characteristics of the soil and Direct shear examination also have been done for the determination of shear strength parameters (Angle of internal and friction Cohesion) and (c) the stability analysis of site 7 using Geostudio Slop W software.

1.7. Structure of the study

This research study is structured into five chapters, each covering specific topics outlined below. The first chapter provides an overview of the research background, including the problem statement, research questions, study objectives, significance, and the scope and limitations of the study, the second chapter focuses on a literature review regarding Roadway Embankment failure. In the third chapter, we discuss the materials and methods used. The fourth chapter presents the results and discussions, are carried out asper the standards and specifications. And the last is chapter five, a conclusions and recommendations are derived from results and discussions.

CHAPTER TWO

2. Literature Review

2.1. Definition of Embankment fill

Select materials that have been deposited and compacted in accordance with engineering criteria are known as embankment fill (Omar et al., 2019).

The primary factors contributing to external loading, which arises from continuous traffic interactions, as well as geohazards such as rainfall erosion and earthquakes. outweigh the resisting forces from soil shear strength, and therefore embankment road failure is inevitable. Driving forces shape the slope failure type: either as shallow or deep, through embankments as a significant slope failure type (Singh et al., 2017). Shallow failure is called gullying, where failure occurs at the slope surface. Deep failure is that which happens well within the slope, where soil chunks flow (Aqib et al., 2023).

2.2.Types of Slope Failures

A slope of earth is an inclined, unsupported surface of a soil mass. The failure of a mass of soil located under the slope is termed a slide or slope failure and constitutes the downward and outward movement of the whole soil mass that participates in the failure (Anand M Hulagabali, K P Deepdarshan, Mahesh P Shetter, Chetan S Gowda, 2020).

Falls

When a chunk of any size breaks loose from a steep slope or cliff, it glides down a surface with minimal shear displacement. It then makes its way through the air, either by free fall, bouncing, or rolling. These movements can occur quite rapidly and might be preceded by smaller shifts that cause the mass to detach from its original position (D.J. Varnes, 1978). A rock fall specifically refers to a mass that has recently broken away from a bedrock area, while debris fall describes the descent of loose material that has come apart before it fails.

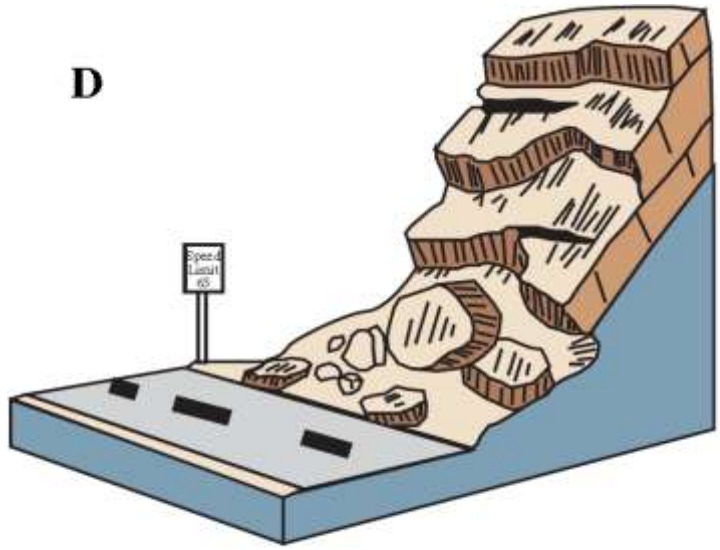

Figure 2.1: A rock fall(Varnes, 1978)

Topping

When we talk about rock masses, toppling failures often occur in areas where there are significant discontinuities—like bedding or foliation—that align with the slope and tilt inward. This kind of failure is pretty common in both natural and man-made rock slopes, such as those formed during the construction of hydropower stations, open-pit mines, railways, and various engineering projects. You can usually break down rock slope toppling failures into three categories: block toppling, flexural toppling, and a mix of both block and flexural toppling (Guo et al., n.d.).

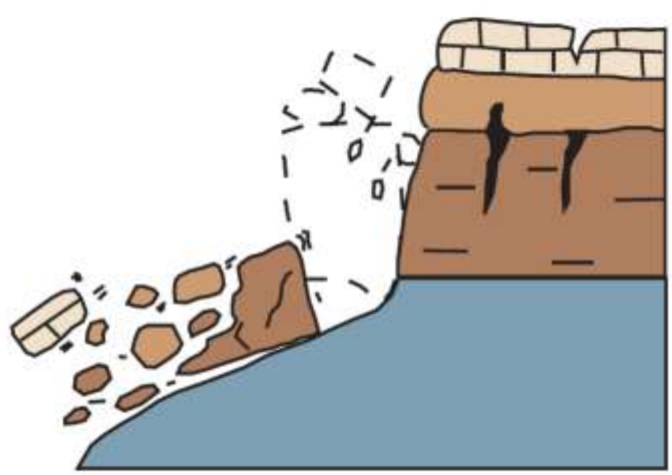

Figure 2.2: Topple(Varnes, 1978)

Slide

When we mention "landslides," we're typically talking about certain kinds of mass movements. This term usually refers to scenarios where a noticeable weak spot allows the sliding material to detach from the more stable ground underneath. The two main types of slides are translational slides and rotational slides (Landslides, 2004).

Rotational slide

This slide features a surface of rupture that curves upward in a concave shape, and the movement of the slide is primarily rotational around an axis that runs parallel to the ground and crosses the slide.

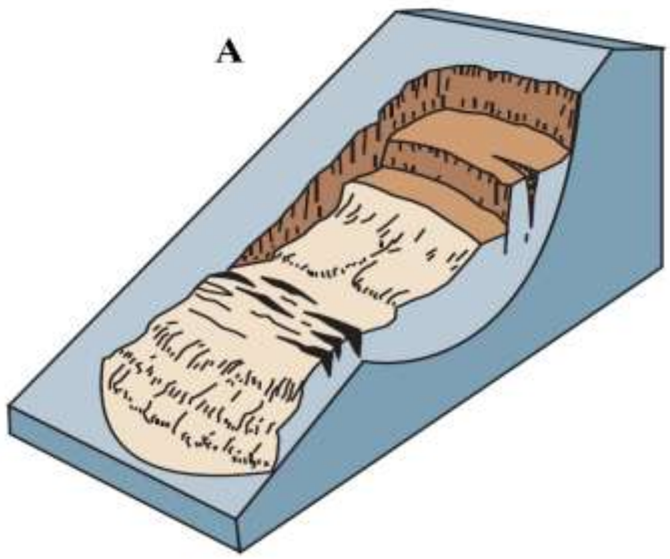

Figure 2.3: Rotational slide parallel to the ground(Varnes, 1978)

Translational slide:

In this kind of slide, the mass of the landslide glides smoothly over a mostly flat surface, showing little to no rotation or backward tilting. A slide like a block is a particular kind of translational slide where the moving mass is made up of either one large piece or a few tightly connected chunks that slide down the slope together as a single unit.

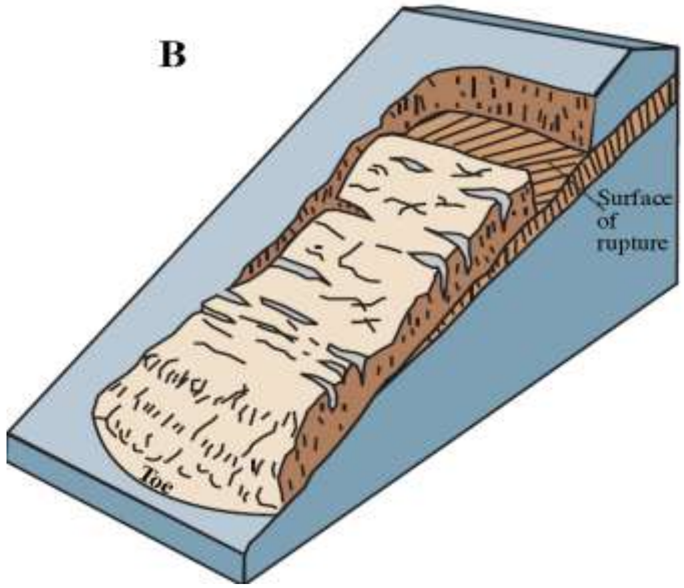

Figure 2.4: Translational slide over the flat surface(Varnes, 1978)

Flows:

There are five basic categories of flows that differ from one another in fundamental ways.

A.Debris flow: A debris flow is essentially a fast-moving mix of materials that combines organic matter, loose soil, rocks, water, and air into a thick slurry that rushes down slopes. Typically, these flows contain less than 50% fine particles. They often occur when there's a significant amount of surface water, which can be triggered by or rapid snowmelt or heavy rainfall that washes away rocks from steep hillsides or loose soil. Debris flows may also be triggered by other landslides. on steep, nearly saturated slopes, especially if they have a lot of silt and sand-sized particles. You’ll usually find the beginnings of debris flows in steep gullies, and the deposits they leave behind are often characterized by broken pieces of sediments at the mouths of these gullies. It’s also important to note that wildfires that strip away vegetation can make these slopes even more susceptible to debris flows.

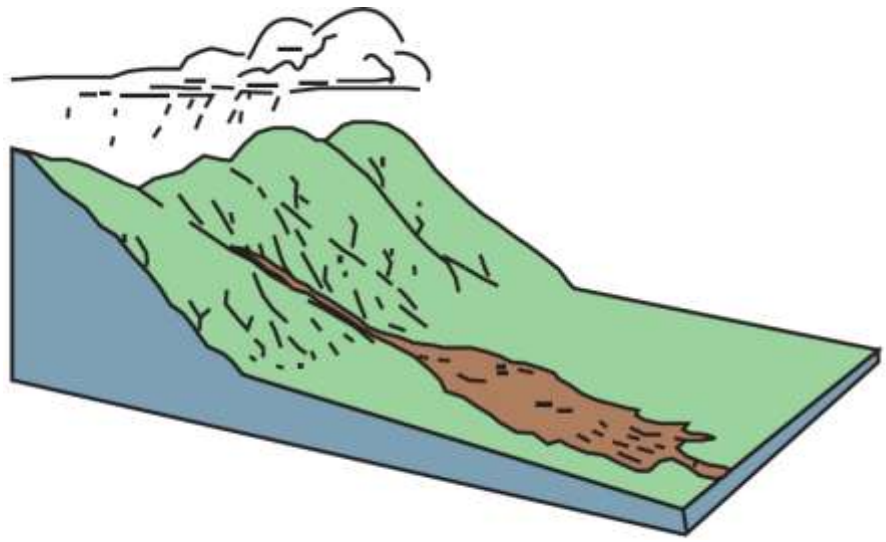

Figure 2.5: Debris flow of organic matters(Varnes, 1978)

b. Debris avalanche: This refers to a range of debris flows that can occur at speeds from very fast to incredibly fast. .

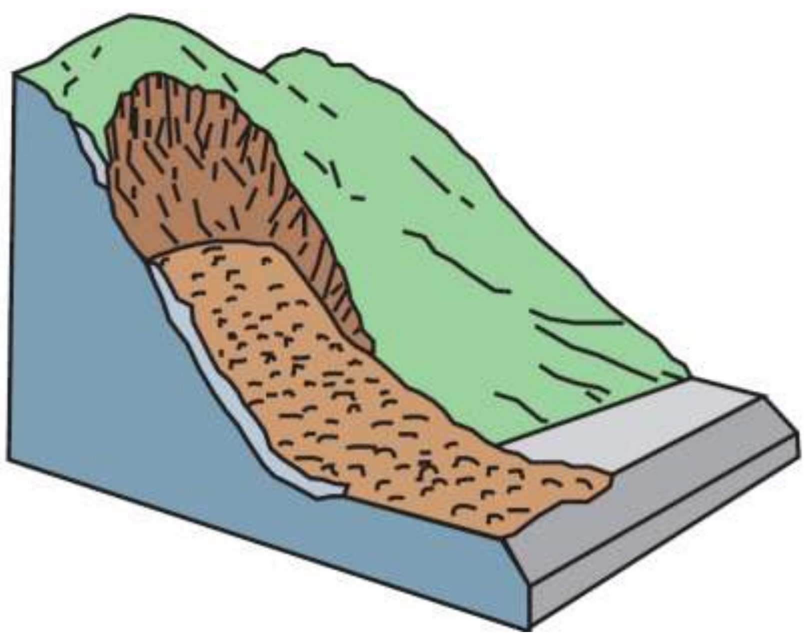

Figure 2.6: Debris avalanche flow(Varnes, 1978)

c. Earth flow: Earth flows are well-known for their distinctive “hourglass” shape When the material on a slope becomes liquid, it spills out, creating a round or depression at the top. These flows typically spread outward and are most often found in fine-grained materials or clay-rich rocks on moderate slopes, especially when the ground is saturated. That said, it’s important to mention that dry flows can also happen, which consist of granular materials.

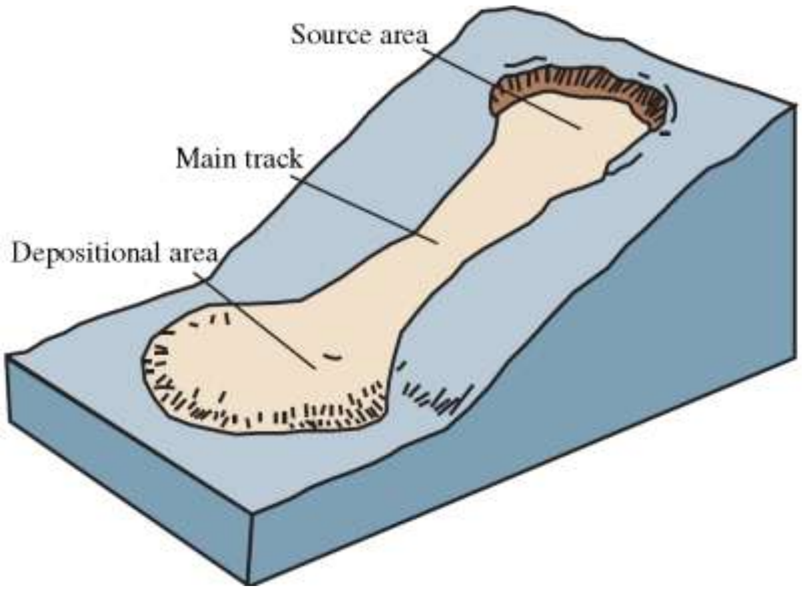

Figure 2.7: Earth flow of a material(Varnes, 1978)

d. Mudflow: A mudflow is essentially a type of earth flow that happens when the material is so saturated with water that it can move quickly. It's made up of at least 50 percent particles like sand, silt, and clay. You might have noticed that in some news articles, mudflows and debris flows are often called "mudslides."

e. Creep: Creep refers to that slow, almost sneaky movement of rock or soil sliding down a slope. It occurs when the shear stress is strong enough to create some lasting changes, but not quite enough to trigger a complete failure. Generally, creeps are classified as: (1) seasonal creep, which is influenced by moisture and temperature changes throughout the seasons; (2) ongoing deformation, where the shear stress persistently surpasses the material's capacity to withstand it; and (3) progressive creep, which occurs when slopes are nearing failure, frequently taking place in conjunction with other mass movements. You can usually spot creep by looking for tilted retaining wall, bent fences, curved tree trunks, tilted poles, and those little ripples or ridges in the soil.

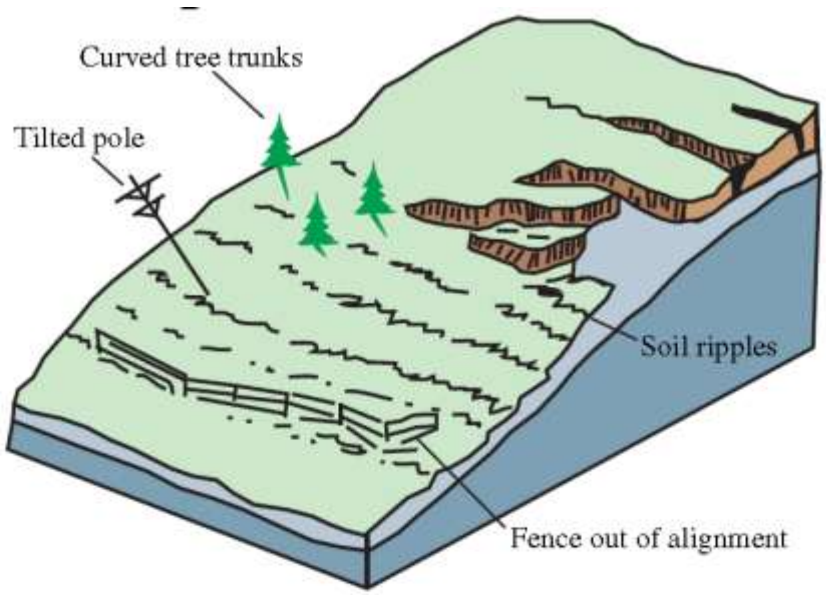

Figure 2.8: Creep movement of a soil(Varnes, 1978)

Lateral spreads:

Lateral spreads are really intriguing because they tend to happen on gentle slopes or flat ground. They mainly move through lateral extension, often paired with shear or tensile fractures. This kind of failure occurs due to liquefaction, which is when saturated, loose, cohesion less sediments—usually sands and silts—shift from a solid to a liquid state. These failures are often triggered by quick ground movements, like those during an earthquake, but human activities can also contribute. When solid materials, whether its bedrock or soil, sit on top of liquefiable materials, the upper layers might crack, stretch, and then subside, shift, rotate, break apart, or even liquefy and flow. On shallow slopes in fine-grained materials, lateral spreading tends to develop gradually. It frequently begins unexpectedly in a limited space and then rapidly expands. Typically, the first sign of failure is a prolonged, but sometimes movement can occur without any clear reason. When two or more of these types come together, it’s referred to as a complexlandslide.

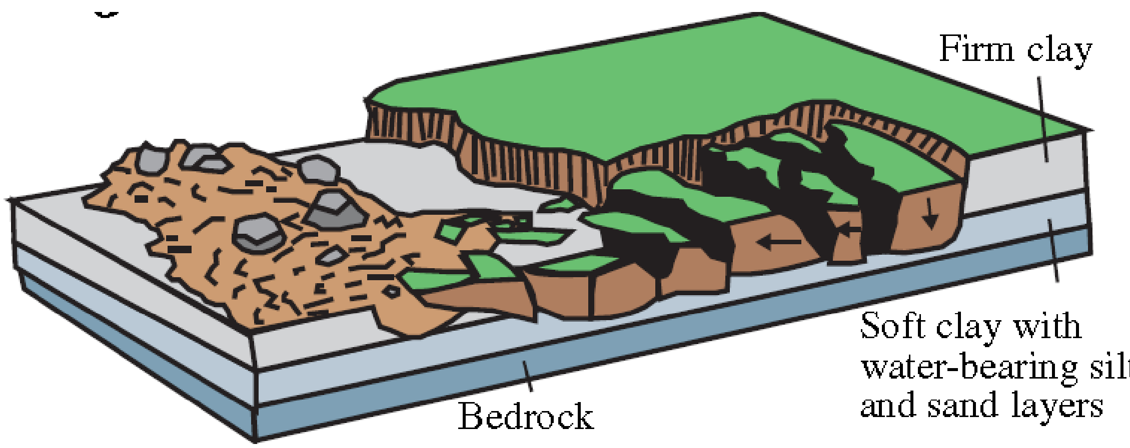

Figure 2.9: Lateral spread of a flat ground(Varnes, 1978)

2.3. Factors Affecting Slope Stability:

Geologic/Geomorphic factors

Poor structural characteristics, such as weak or soft rock Constraints, unfavorable bedding sequences and undesirable structure predisposes some of the terrain to soil mass movement. Weakology types are a mark of weathering as well as relative strength of the geologic material. Deep, clayey soils which are susceptible to deep-seated soil creep and earth flows develop in deeply, windward-slanting land in the wet, piedmont areas for high rainfall sedimentary and volcanoclastic rocks break down there. The effect of the rocks structures (bedding planes, fold, joints, faults, etc. is an important condition of the natural slopes stability. Fault zones often contain fractured, crushed, or otherwise metamorphosed rocks as a result of release of stress and intrusion of igneous or ultramafic rocks into geologic uplift. Clay soil between the soil-bedrock interface is likely to be vulnerable to such surface failure as sliding-type (Swanston 1984).

Slope Shape

Shape of slopes is critical in the assessment of soil water distribution in unstable landscapes. Legend slopes distribute subsurface water and are more stable compared to concave slopes that concentrate subsurface water in small points of the slope. Therefore, soil in hill slope depressions, may one be much thicker than in intervening minor ridges, which would further increase the likelihood of additional failure.

Vegetation

Effects of Roots on Stability of Slopes Hill slope stability is affected positively and negatively by different root systems on the hill slopes. Root and rootlets are thus anchoring vertically through the soil mantle, into fractured bedrock or other more stable substrate, increasing the strength of the soil. This mechanism is effective only in stabilizing rather thin soils (i.e. <1 m), such as on steep.

Earthquakes

The outcome of the earthquakes is a phenomenon of dynamic forces especially dynamic shear forces reducing shear strength and stiffening of soil. The pour water pressures in large gravel saturated soils may reach the total mean stress and treat the soils as if they were viscous fluids a process called dynamic liquefaction. Carcasses on top of such soils would fall, carcasses under them would rises. The process rate (a few seconds) at which the dynamic forces are generated, preclude coarse grained soils from eliminating the excess pore water pressures. Even so, seismic failure even is common in the undrained condition (Jamaludin, 2011).

Ground water

Geology affects the flow of groundwater, its direction, pressure and gradient at any point below any given slope. Water can affect the strength of the materials by (i) chemical alteration and solution, (ii) reduction of apparent cohesion due to capillary forces which disappear on submergence or saturation, (iii) increasing pore water pressures with consequent reduction of shear strength (iv) the mechanism of softening particularly applicable to strength reductions in stiff-fissured clays as discussed by Terzaghi (1936, 1950) and Terzaghi and Peck (1967). As previously mentioned, the increase in pore water pressure resulting from groundwater movement is a crucial factor in causing slope instability and landslides. Importantly, pressurized groundwater frequently acts as a primary contributor to significant failure incidents. Commonly contributes to extreme slides of the flow type (Analysis, n.d.).

Weathering

Depending on weathering, Blyth and de Freitas (1974) report that chemical changes are capable of happening very rapidly (e.g. within a few days). The speed at which this reduction takes place is affected not only by the makeup of slope materials but also by climatic conditions, drainage characteristics, and geological factors. According to Terzaghi and Peck (1967), the cohesion present in shales is considerably more important than the impacts of chemical weathering. This is because geological processes—such as the removal of overburden—can disrupt internal bonds through networks of joints, often reaching much deeper than chemical weathering can. Furthermore, geological features such as joints, bedding planes, and faults significantly influence the formation and characteristics of the weathering profile (Analysis, n.d.).

Slope Stability Analysis

A slope is a ground where one end is elevated in levels compared to the other. A rising or falling ground. An earth slope is an unconsolidated sloping surface of a mass of soil. A slide is failure of a mass of soil below slope; that is, the entire mass of soil thrusts itself off and down.

Gravitational and seepage forces in the soil are major contributing forces responsible for slope failures (Anand M Hulagabali, K P Deepdarshan, Mahesh P Shetter, Chetan S Gowda, 2020).

Limit equilibrium

Invented by Coulomb in 1773 as a geotechnical concept, limit equilibrium is the oldest methodof undertaking stability analysis. This technique (in its simplest form) assumes a failure mechanism and implicitly by the conventional strength parameters C and Ø imposes constraints on the loads on the failure planes. Suppleness and longevity are primary advantages of the limit-equilibrium method causing easy-to-use software and a range of common knowledge about its reliability. However, its main weakness is, that one will need to come up with educated guess about the overall shape of the failure surface in advance. Incorrect decisions lead to incorrect attempts to predict failure load (Sloan, 2013).

Establishment of mostly limit equilibrium methods are based on the slices method. Figure 1 presents a general form of such methods.

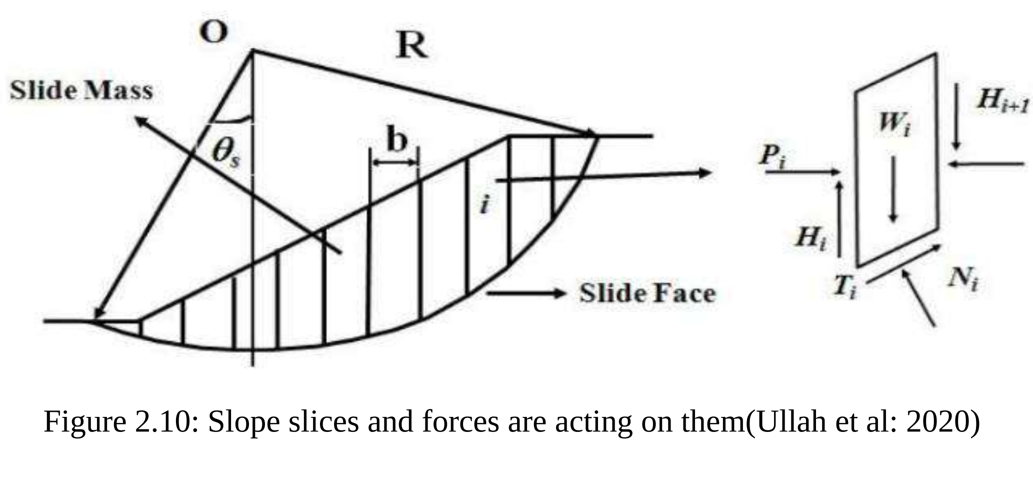

Figure 2.10: Slope slices and forces are acting on them(Ullah et al: 2020)

Selective preservation of some of these slices by Ullah et al (2020) is as follows:

An equilibrium sliding body (i.e one safety factor incorporated in the failure mass), the slipping surface strength is varied accordingly.

• Inter-slice forces are considered in the case of specific problem determination.

The sliding mass over the failure surface can be divided into a number finite slices, slices are commonly sectioned vertically, however, in some works, inclined or horizontal cuts are taken.

Other value of the safety factor may be found on the basis of the equations of force or moment equilibrium.

Limit equilibrium techniques; Include methods of slices Bishop's method corrected, force equilibrium methods and Janbu's method based on generalised processes of slices, (Morgenstern & price) and Spencer's method. Soil /Rock bulk should be sliced up as a matter of course using these techniques. It is an advantage to use Continuance surface of the soil mass to exercise the soil mass of limit equilibrium methods. In order that one gets the form equations of equilibrium in these procedures, one must be making an assumption somewhere prior to the calculations, like side force orientation, before getting the equations of equilibrium (Nuricetal. 2013a).

Limit equilibrium techniques encompass: the Ordinary method of slices and the standard (Bishop) simplified method, Janbu's simplified and generalized method, Morgenstern Price's method, Spencer's method, as well as force equilibrium methods (Nuric et al 2013 b).

Ordinary method of slices

The other name for Ordinary Method of Slices is Fellenius method or Swedish circle method. Only circular slip surfaces can use it. The moment equilibrium equation of entire mass is satisfied.

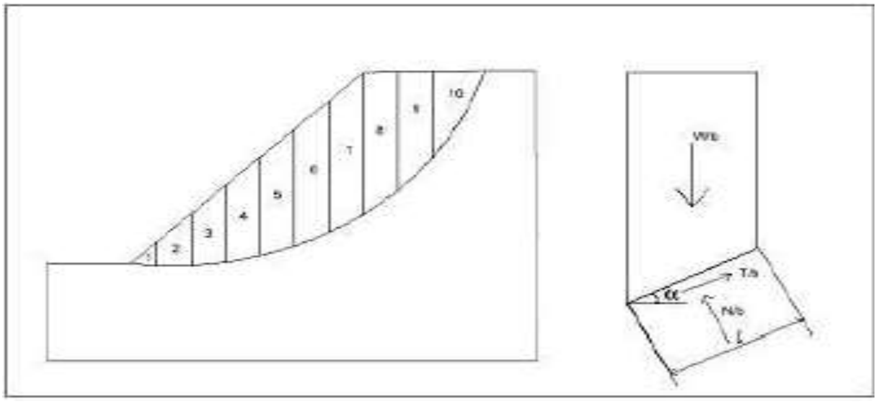

Figure 2.11: Ordinary method of slices(Nuric et al: 2013 b).

Bishop’s method

Approach that did not consider the interstice shear forces, but, took the interstice normal forces into account, was developed in the 1950s by Professor Bishop of Imperial College in London. Bishop’s approach only satisfies moment equilibrium. Bishops fractures approach is almost having power equilibrium when the interstice normal forces are considered, from the force polygon for each slice. From the vertical summation of slice forces, Bishop obtained an equation for normal at the slice base As a result, the component of the Factor of Safety (FOS) is determined by the safety factor. This creates a non-linear aspect in the safety factor equation since the FOS appears on both sides of the equation, necessitating the use of an iterative method to compute the safety factor.

Spencer's method

Spencer's approach meets every equilibrium requirement. It works on any kind of slick surface. It makes the assumption that each slice's side force inclinations are the same. In order to ensure that all equilibrium requirements are met, the side force inclination is computed throughout the solution procedure. It is a precise technique.

Morgenstern-Price Method.

This approach is developed by Morgenstern and Price (1965) and spencer (1967) not only on normal and tangential equilibrium but also in the moment equilibrium of each slice with circular and non-circular slip surfaces The safety factor is established through an optical design methodology that entails the summation of both tangential and normal forces at the base of a slice, in addition to computing the total moments around the center of the base. These equations were formulated under the assumption that the slice possesses an infinitesimally small width. To achieve equilibrium for both forces and moments, the relevant equations were resolved utilizing an advanced Newton-Raphson numerical method. In determining the cumulative impact of interslice shear and normal forces (Hajiannia and Noroozi, 2015), a hypothetical assumption was required due to the challenges in directly specifying their resultant.

Fellimens Method

Type rotational slip is assumed in this method as can be seen from Fig. 5. Further, landslides soil is segregated in to sometime slices to determine moment around the critical circle. Anyhow, there are some parameters that shall be calculated in the following ways: R is radius of critical circle (m); C is Cohesion (kN/m2); and u is angle of shearing resistance; W is weight of each slice (KN); α is angle between horizontal axis and the bottom of slice (degree); L is the length of the failed land slide (m). Factor of safety (F) can be approximated in the following formula (Hajiannia & Noroozi, 2015).

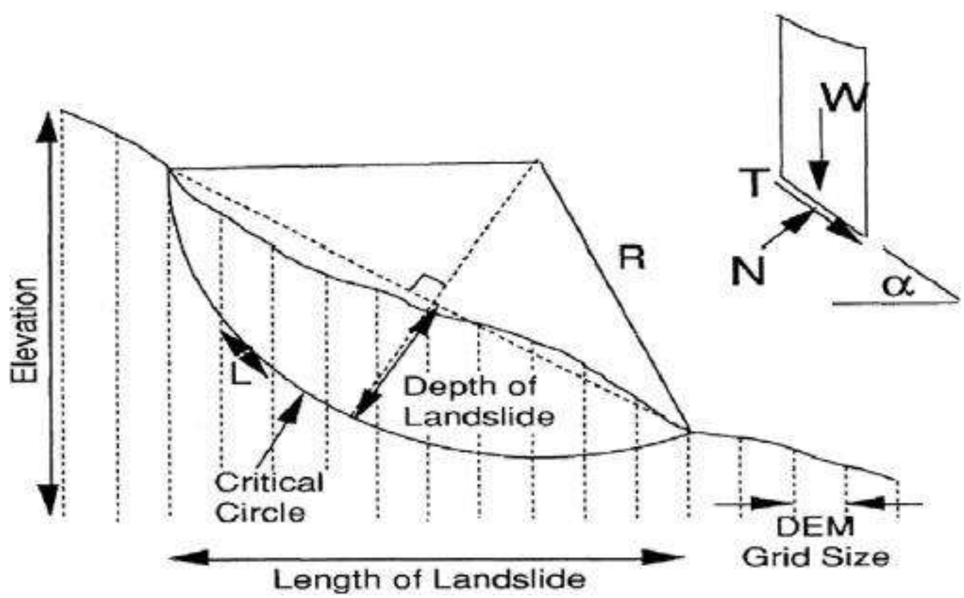

Figure 2.12: Fellinnens method(Hajiannia & Noroozi, 2015).

2.4. Geostudio/slope/w

Created by GEO-SLOPE International Ltd. in Canada, SLOPE/W is a powerful software tool grounded in limit equilibrium theory, designed for the assessment of slope stability. It assesses the safety factor over various possible slip surfaces, which encompass circular, non-circular, and custom-defined shapes (SLOPE/W 2002; Krahn, 2004). While it automatically searches for circular slip surfaces, the circular critical slip surface (CSS) is determined using the same general input parameters as the slope, with the entry and exit search options validated through the auto-locate feature. The analysis employs the Mohr-Coulomb soil model and failure criteria, along with a half sine function to account for interslice forces, ultimately calculating the factor of safety from the critical slip surface (R. Desai & R. Joshi, 2019). Since its inception in Canada in 1977, GeoStudio has evolved into a comprehensive software suite for geotechnical modeling and analysis, tackling challenges related to soil structure reinforcement, deformation analysis, and soil stability. During the analysis, the properties of structural components can be integrated into the stress deformation analysis, allowing for the calculation of forces and moments within the structure, as well as the interaction between the structure and the soil. Stability analysis can be performed considering all or part of the structural load components applied to the shear mass, and users have the flexibility to include or exclude structural components to better reflect real-world field conditions (Panda & Behera, 2021).

Slope/W is a key part of GeoStudio. In this research, we analyze slope stability using methods like Fellenius, Bishop, and Janbu, all within the GeoStudio (Slope/W) software. The traditional Limit Equilibrium method serves as the backbone for calculating slope stability in the GeoStudio (Slope/W) Program. This method is based on moments and determines the safety factor by balancing the moment equations. Here, the factor of safety is determined as the ratio of the available shear resistance to what is needed for equilibrium.

For decades, limit equilibrium analyses have been a staple in geotechnical engineering for evaluating slope stability. The SLOPE/W software (GEOSLOPE 2010) tackles slope stability challenges using various methods, including Bishop's Modified method, Janbu's Simplified method, Spencer method, and the Morgenstern-Price method (M-PM), among others. These analyses aim to identify the lowest factor of safety (FS) for slopes, which helps us understand how close they are to failure. SLOPE/W is part of the broader GeoStudio suite of geotechnical tools, built on limit equilibrium principles and designed as an intuitive finite element tool for slope stability analysis (Ghosh, 2019).

2.5. Land slide Mitigation Strategies

Regarding to Slope

Sometimes, tackling an unstable slope can be surprisingly simple: just think of it as a less steep incline. By easing the steepness, you can also reduce the damaging effects of the surface water inside it.

Grading is just the act of shifting soil from one place to another. If there is enough horizontal space, making the slope less steep is the easiest solution.

That said, remember that adjusting a slope isn't always possible—especially if you're dealing with a steep slope in a cramped area where there's not much room to work with. In those situations, you might need to look into other methods for stabilizing the slope instead (Brian Dalinghaus, 2025).

Adding Drainage to the Slope

One great way to tackle the erosion that can happen on your slope is by setting up a drainage system. Since flowing water is a major culprit behind slope instability, having a drainage solution is one of the smartest moves you can make. As water cascades down a hill, it gains speed and becomes more effective at causing erosion. The longer the slope, the more time and distance the water has to ramp up its speed and the damage it can inflict. By installing a drainage channel, like a French drain, along the length of your hill, you can effectively redirect that water away from the slope. Using a French drain to catch surface water partway down the slope can significantly lessen the erosion that occurs with each rainfall (Brian Dalinghaus, 2025).

Plantation the Slope (Vegetation)

One of the best ways to keep a slope stable is by planting it. The roots of plants are fantastic at gripping the soil as they grow, helping to hold everything in place. You'll notice that some plants are better suited for this task than others. For example, creeping ground covers, turf, and vines are all great choices for planting on slopes. Plus, it's a good idea to incorporate plants into any other measures you take for slope stability. Letting those plants spread out over the slope can significantly reduce the chances of erosion messing with your soil down the line (Brian Dalinghaus, 2025).

Building a Retaining Wall

Our next approach to stabilizing slopes might take a little longer and could cost a bit more, but it's one of the most effective solutions available. Retaining walls are excellent at holding soil in place and can surprisingly bear a lot of weight. On top of that, they assist with drainage in the surrounding area, which is a fantastic perk. Building a retaining wall is no easy feat, so it's a good idea to hire a professional team with the right construction expertise to make sure it's done right. For slopes that are unstable, a well-constructed retaining wall is definitely the way to go (Brian Dalinghaus, 2025).

2.6. Summary

This literature review has examined the various causes, mechanisms, and assessment methods associated with road embankment failures. Key contributing factors include rainfall, seismic activity, construction defects, and subsurface variations. Common failure mechanisms involve slope instability, liquefaction, seepage, and erosion. Essential tools for characterizing and assessing embankment stability include in-situ testing, geophysical surveys, laboratory testing, and numerical modeling. There are several mitigation and remediation strategies available, such as soil stabilization, ground improvement, drainage enhancements, and modifications to embankment design, all aimed at improving stability. Despite notable progress, there are still research gaps, especially in understanding how multiple failure mechanisms interact, enhancing numerical modeling capabilities, and creating advanced monitoring and prediction techniques. Future research in these areas will be vital for enhancing the safety and resilience of road embankments and ensuring the sustainability of transportation infrastructure.

CHAPTER THREE

3. Materials and methods

3.1. Location of the study area

Bako-Shambu Road is located in Oromia Regional State and is approximately 230 km long from the west of Addis Ababa.Its latitude and longitude were 9^0 08'N and 37^0 03'E, respectively, and its elevation is 1743m above sea level.The project road connects Bako and Shambu towns. It runs nearly to north direction from Bako town through Jera and Haretao village to reach Shambu town.

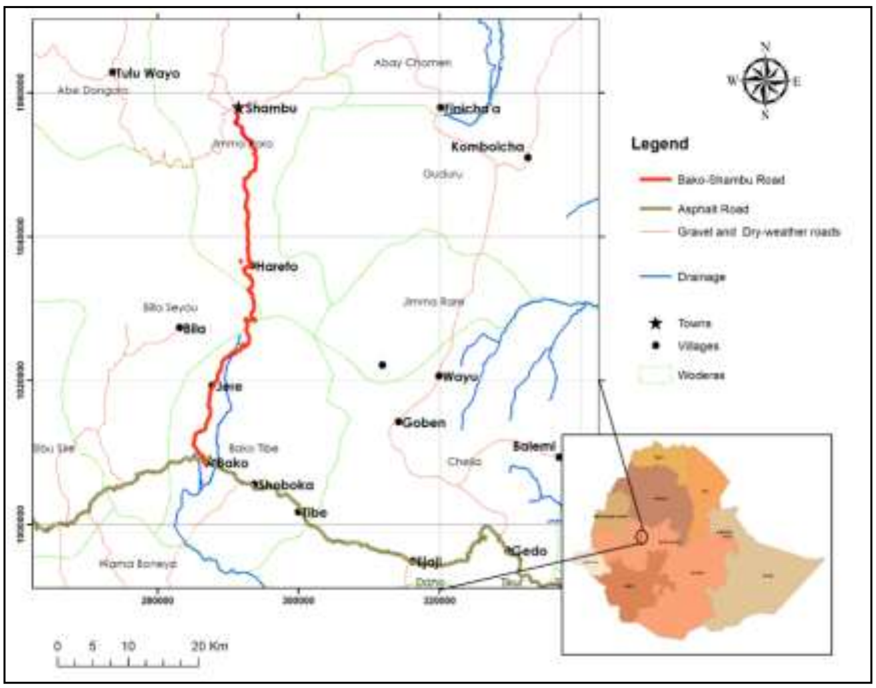

Figure 3.1: Location map of the Bako-Shambu project

3.2. Research Design

In order to achieve the research objectives, different methodologies will be employed. This includes, Problem identification, Literature review, Field investigation, data collection, Soil sampling, Laboratory testing, Slope stability analysis, Results and discussions and, conclusion and recommendation.

The Research approaches that are used in this study were, experimental, analytical and field-based, as well as qualitative and quantitative data’s were used.

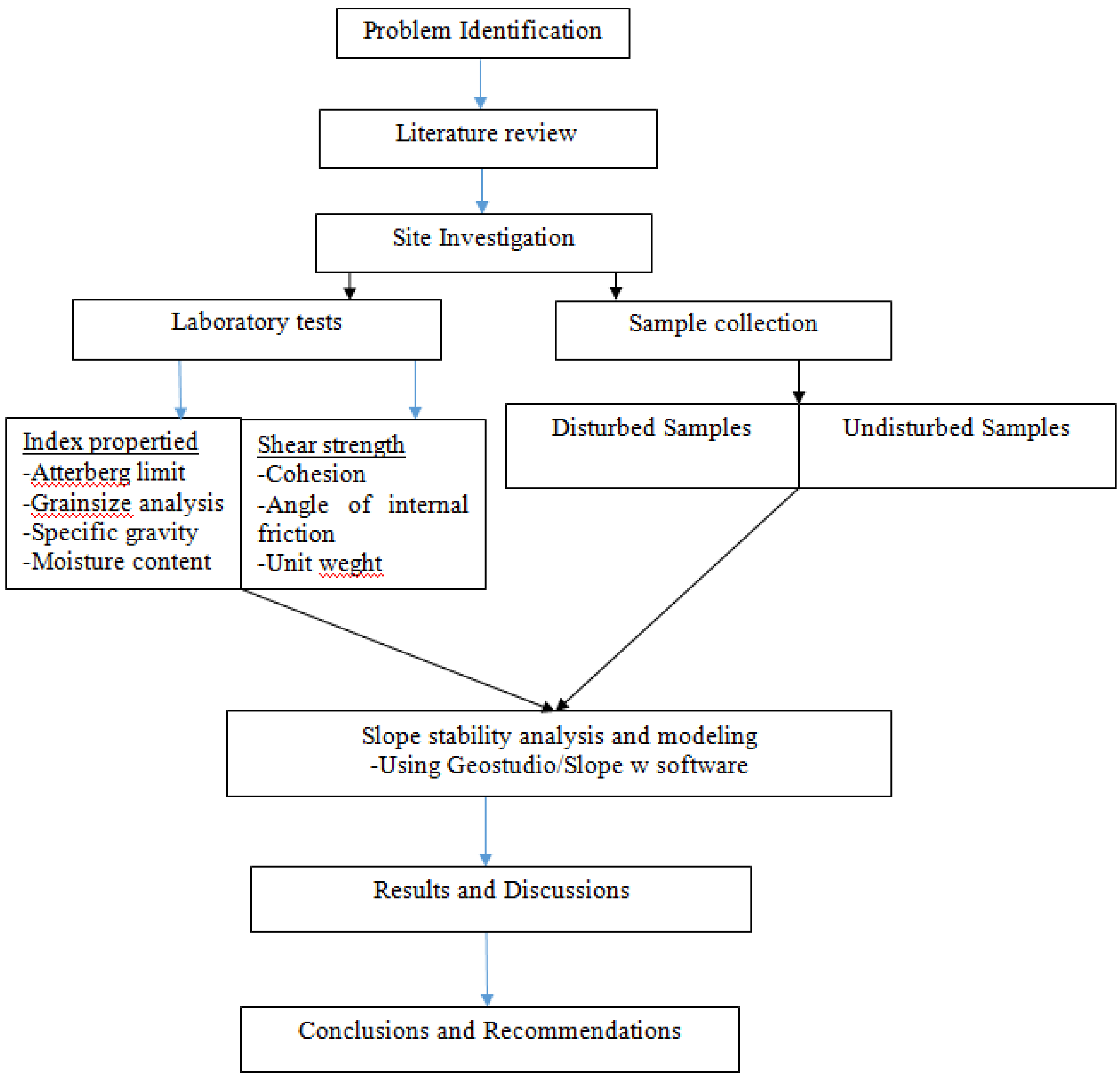

Figure 3.2: General Research Design and Flow Chart of Methodology

3.3. Field Investigation

3.3.1. General

Landslides and slope failures primarily take place along the southwestern escarpment of the volcanic landscape in the main highlands of southwestern Ethiopia. This area is noted for its steep terrain, significant rainfall, and shallow groundwater sources like springs. It is well-known for its vulnerability to landslides, mainly as a result of a mix of geological and geomorphological factors that encourage slope instability. The factors contributing to this include the type of rock, soil formation, climatic conditions, terrain characteristics, and the presence of both surface and subsurface water.

3.4. Site Characterization

Site 01 (km 94+160 – km 94+210)

This section is affected by a side slope failure in LHS for about 50m. Its regional landform shows that the area is within the old slides zone, where the back slope had been slide down from its parent hill. It also shows some tension cracks in RHS for a possible progressive failure in back slope indicating the movement is deep seated. The affected road section is a straight section of the alignment that is oriented nearly N-S, and located south of Hereto town.

The failure is a typical circular embankment failure (Km 94+150-94+220) that is associated with toe erosion and saturation by the near river found in LHS within old landslide zone. The embankment failure caused back slope slump and tension cracks in the RHS with nearly equivalent slip and displacement indicating the direct response of the embankment failure. The erosive river coming from the RHS mountainous section crosses the road with slab culvert at Km 94+300. It is causing intensive erosion starting from the outlet and already removed the protection masonry wall at the outlet and keeps aggressively eroding both river banks as shown in the photo below. The river bank is constituted by in the thick residual soil, representing the sub grade nature of the failure section. There are minor surface flows from mountainous section as a sheet flow, and creating a water logging in the RHS to saturate the fill; and the more pronounced surface flow is also found at around Km 94+220 causing water logging in the RHS to saturate the failed section.The actual failure mass extended to the river side and failed mass width is 40m and extends not far from 50m on average from the detachment (failure) to the river bed with about 10-15m elevation drop to river bed.

Figure 3.3: The typical rotational embankment failure at Site-1(Reference Author)

Site 03 (km 97+800 –km 97+880)

This section is affected by a side slope failure, which is associated with typical rotational fill embankment failure, in LHS for about 80m and associated with toe erosion and saturation by the river found in LHS.Furthermore minor pavement distress also noticed between km 97+910 to 97+940 at the sharp curve section that might be related with subgrade saturation. The area is constituted by soft, wet and erodible residual soil and moderately sloping side slope. It is affected by river erosion, which is also fed by the turnout flash from the road ditch. The river caused huge riverbank mass movement that is triggered by its intensive erosive nature to that of the soil's erodibility. The river action further caused the embankment failure which is founded on the weak formation where regular saturation is common. The failure is bounded by river in the west. The road is situated in the lower volcanic that has a thick reddish residual soil formation.

Figure 3.4: The typical rotational embankment failure at Site-3(Reference Author)

The actual failure mass extended to the river side width is 120m and extends in to the river 40-110m from the detachment (failure) to the river bed with about 20-25m elevation drop to river bed.

Site 05 (km 99+660 – km 99+760)

This section is affected by fill embankment failure, in LHS for about 100m at the descending section from the ridge top towards north into the Omo river basin. It was constructed on the loose, unconsolidated sediments.

In this section, the road is an embankment fill section with a fill height of about 5.0m and

1.5H: 1V side slope ratio. The circular minor edge embankment failure (Km 99+660-99+700) that is associated with possible toe erosion and saturation by the nearly river found in RHS about 80m showing progressive eroding the toe and gets closer to road with time. However, the river is bit far and also the failure slip boundary remains in embankment boundary and the initiated in tension cracks in the side slope is not continuing to the river and remains with the soil mass within 10-15m range both side of the failed section.

The erosive river runs parallel to the side of the road in the RHS and get closer only in the failed section with about 80m. It is causing intensive erosion at the toe and meandering. The actual embankment failure limited in the fill section and the tension cracks in the side slope limited to 10-15m. The moved mass width is 50m and extends not far from 15m on average with about 7-10m elevation drop to the tension cracking ends the embankment is constructed up on the loose, unconsolidated sediments. The RHS of the road is relatively lower elevation and covered with swampy brown soil mixed with gravel, volcanic boulders and clay matrixes. The soil is weak and affected at the base by the erosive river that located west about 80-100m away from the centerline.

Figure 3.5: The typical rotational embankment failure at Site-5(Reference Author)

Site 06 (km 99+800 – km 99+860)

This section is affected by fill embankment failure, in RHS for about 60m. It was constructed on the residual soil formation. The failure in this sections showed a typical circular/rotational embankment failure. It has been reported that the road suffered embankment slip failure in RHS that has been reconstructed; however, it is still failing again.

The road traverses to SE direction, crossing gently sloping hill within the mountainous section. The LHS is the hill section the dips in gentling sloping (80-150) to the RHS along a side hill. In this section, the road is an embankment fill section with a fill height of about 4.0m and 1.5H: 1V side slope ration. The reconstruction also included an infiltration gallery constructed in the LHS to a depth 4.0m below the subgrade level to intercept and guide the subsurface flow to drain in the pipe culvert at 99+910. In addition, masonry retaining wall constructed on RHS with a total height of 4.2m with only 1m extending above the surface and placed on 1.0m rock fill at RHS and founded at 3.3m below the OGL. The embankment material rested on rock-fill of 1m below the OGL with a minimum of 3% slope. Geotextile also placed on top of the rock-fill before the placement of embankment/fill material.

Figure 3.6: The typical rotational embankment failure at Site-6(Reference Author)

The erosive river runs parallel to the side of the road in the RHS and get closer only in the failed section with about 150m. It is causing intensive erosion at the toe and meandering .The actual embankment failure caused serious side slope failure due to the spoil loading river toe erosion. The failed mass width is 120m and extends far to the river from about 100-150m with about 15-20m elevation drop.

Site 07 (km 104+050 – km 104+230)

This section is affected by side slope (LHS) failure that affected the embankment and pavement, for about 180m. The failure in this section is marked by a typical an embankment failure that is constructed on the residual soil formation.

Major landslide occurred (Km 104+050-104+230) in the LHS side slope caused major detachment and moved the entire mass to 8.0m down-slip of 90m*100m long. The major detachment is nearly at the center of the road where about 8m down-slip is observed; and there is no tension crack mapped in the RHS indicating that the road at the current condition seems stable. There is no any deformation in the telecom tower in the RHS that is only 45m away the head of the landslide. .

Before the major failure, the section suffered minor embankment failure marked by longitudinal crack on the pavement; and which later gets the major detachment failure crown. There was a side slope failure around Km104+250 in LHS about 50m away.

The major landslide mass width is 100m and extends far in the side slope of about 90m with about 20-25m elevation drop.

The road traverses to SE direction, crossing gently sloping hill within the mountainous sec tion. The LHS is the hill section the dips in gentling sloping (80-150) to the RHS along a side hill. In this section, the road is an embankment fill section with a fill height of about 4.0m and 1.5H: 1V side slope ration. The reconstruction also included an infiltration gallery constructed in the LHS to a depth 4.0m below the sub grade level to intercept and guide the subsurface flow to drain in the pipe culvert at 99+910. In addition, masonry retaining wall constructed on RHS with a total height of 4.2m with only 1m extending above the surface and placed on 1.0m rock fill at RHS and founded at 3.3m below the OGL. The embankment material rested on rock-fill of 1m below the OGL with a minimum of 3% slope. Geotextile also placed on top of the rock-fill before the placement of embankment/fill material.

Figure 3.7: The typical rotational embankment failed at Site-7(Reference Author)

Figure 3.8: The typical rotational embankment failed at Site-7(Reference Author)

Site 09 (km 105+290 – km 105+370)

This section from km 105+290 to km 105+370 is embankment fill and the road shows a total fill distortion, settlement and circular failure caused by the crossing river's erosion and saturation in both the upstream and downstream sides. The crossing river located at km

105+375 is not well channeled and could directly saturate the fill section in the inlet section before it crossing. It also causes severe erosion in the downstream side to saturate the entire river bank as a result foundation of the embankment failure and settlement noticed. The river then turns to the left and runs nearly parallel to the road to cause serious progressive erosion with time. The erode river rims and widening and gets closer to the road to initiate further embankment failure. The failed and settled road segment is about 80m covering the entire width of the pavement. The settlement is in nearly half a meter and moved to RHS direction.

Pavement failures are triggered by saturation related to the crossing and meandering river and as its cause's spills in the flood plain and also water logging to crate swampy sections.

Figure 3.9: The pavement and embankment failures in Site-9(Reference Author)

During the inspection conducted from March to May 2021, the embankment section exhibited signs of instability, which were evident through settlement and a significant longitudinal crack, especially at the center of the road, as illustrated in the photographs. However, no visible mass movement or detachment of slumped material was observed on the road

section.***Site 11 (km 106+540 – km 106+680)***

This section of the failed road associated with river erosion, surface water courses and spoil piling. It caused severely deformation and continuous pavement sliding and failure along gently-sloping road stretch covering about 140m. It marked by pavement sliding/cracking, sliding and overlapping of side ditches between km 106+540-106+580. The overview of the failed embankment fills at Site-11

On the RHS of the road section observed serious of sliding following the direction of the river and turns back to the LHS after crossing at Km 106+780. The big river then caused serious erosion and saturation again in the LHS side which is loaded by the huge spoil pile, and caused major landslide in the LHS. The actual failure mass width in the LHS extended to the river side for about 230m and then it extends again about 100m. Within this river section observed also river bank collapse in many section. Pavement deformations and failures triggered by saturation from the shallow groundwater, rainfall and bank erosion due to the meandering river across and along the carriage way. It is bounded by streams in both sides of the road.

Figure 3.10 side slopes failures at Site-11(Reference Author)

3.5.Detailed Investigation of the Selected Failed Slopes Site 7 (104+140)

3.6.Data Collection

The data collection includes Field investigations, Soil Sampling; Laboratory Tests and Slope stability analysis have been done on the research area which is Bako-Shambu road project especially at Site 7 (104+140) km.In this research the available data’s like metrological data, Google earth images, etc are collected from Google earth image interpretation and Ethiopian national metrological agency.

3.7.Sampling

Using purposive and systematic random sampling methods, both disturbed and undisturbed soil Soil samples are collected to assess the geotechnical properties of the slope materials in accordance with ASTM standard procedures.UN disturbed and disturbed soil samples were collected from top, middle and bottom of the failed embankment section of site 7 (104+140) km at a depths of 1m, 5m and 9m.

Undisturbed Sample

The undisturbed collected samples using cylinder tube and tied to plastic bag to prevent moisture loss was used for Direct Shear test for the determination of Shear strength parameters and in situ natural moisture content. The UN disturbed samples were collected from top, middle and bottom of the failed embankment at a depths of 1m, 5m and 9m.

Figure 3.11: Sample of Undisturbed Soil at different depths of Site 7 at station104+140

Disturbed soil samples

The Disturbed samples were also collected from top, middle and bottom of the failed embankment at a depths of 1m, 5m and 9m. And index and engineering properties of soils including liquid limit, plastic limit, plastic index, moisture content, unit weight soil classification, specific gravity were determined.

Figure 3.12: Sampling of Disturbed Soil at different depths of Site 7 at station 104+140

3.8.Laboratory Soil Testing and Procedures

Water Content Determination

The test samples taken from the study area were dried in an oven at 105 °C temperatures in order to determine their The natural moisture content is determined in the laboratory following the ASTM D2216 testing methods. To avoid errors, three sets of samples were generated for each test sample. A suitable sample size was taken for the purpose of determining the moisture content. The three sets of sample natural moisture contents were then determined.

Specific Gravity Determination

Oven- dried representative samples have been collected from the study area for testing sieved over a No. 10 sieve with a 20 gm sample. According to ASTM D854 testing procedures, for three trial samples were taken the soil taken from the study area to conduct this test and the average value was taken.

Determination of Unit Weight of Soil

By inserting a cone cutter into the soil, this test can be used to determine the in-situ density of undisturbed soil. The bulk density is the product of the volume of the soil sample divided by the mass of the moist soil, and the dry density is the product of the volume divided by the mass of the dry soil. The weight of the unit is established through measurement. a) The weight of the vacant cone cutter was recorded, b) the mass of soil sample within cone cutter, and c) the mass of the sample and the cone cutter. From the recorded data, the soil specimen's diameter (D), length (L), and mass (M) were estimated then the soil unit weight has been determined.

Determination of Grain Size Analysis

According to ASTM D422 testing protocols, the laboratory determines the soil grain size analyses for the samples taken. For coarse-and fine-grain soils, respectively, the two most frequent tests utilized were sieve size analysis and hydrometer analysis. In this study, samples were taken from the failed embankment section 7. Given the significant amount of fine-grained materials present in the soil samples, the silt and clay fractions were isolated utilizing the wet sieving method. This procedure entailed washing the oven-dried soil through a 0.075 mm sieve. To facilitate the separation of cohesive, sticky fine particles, sodium hexametaphosphate was employed as a dispersing agent during the hydrometer analysis. Both methods were performed on disturbed soil samples in compliance with ASTM standards D422-63 and

Figure 3.13: During weighting and Sieving of a sample(Reference Gondwana Engineering)

Atterberg Limit

To express the plastic and liquid limitations of a fine-grained soil, the Atterberg limit test was carried out. The ASTM standards and ASTM standards of plasticity charts were used to express the soil type name. The purpose of this test was to determine the soils' structural strength throughout the entire research area.

Determination of Liquid Limit

The liquid limit is the moisture content at which 25 blows. A paste was formed in the evaporation dish by mixing distilled water with approximately 125 g of a soil sample that had been sifted through a 425 micron screen. The paste was divided along the diameter of the cup using a grooving tool, and the number of revolutions required to complete the groove was recorded for a groove measuring about 10 mm in length. The remaining dirt was taken from the cup and combined with the dirt that had previously been spread out on the marble plate.

Depending on the soil's moisture level, more water was added to the mixture or the soil was allowed to dry to vary the consistency. The number of rotations required to seal the groove was counted, and the liquid limit was established in accordance with ASTM D4318.

Figure 3.14: During Liquid Limit determination. (Reference Gondwana Engineering)

Determination of Plastic Limit

It indicates the moisture percentage at which soil can no longer be formed into threads measuring 3.2 mm in diameter without disintegrating. Using the air-dried soil that had been put through a 425 micron screen, the plastic limit was estimated. A ball made of around 8g of the plastic soil was taken and rolled over glass or marble into a thread's diameter dropped to 3.2mm. The ball was rolled into a thread with a constant diameter throughout its length, using just enough pressure to roll it into a ball. The procedure was carried out until the thread's 3.2mm diameter point of collapse. At least 24 hours were given for the plastic substance to develop and become permeable to water.

Figure 3.15: During Plastic Limit determination(Reference Gondwana Engineering).

Determination of Plasticity Index

To determine the range over which the soils in the study areas stay plastic before deformation, the PI was computed using liquid and plastic limits.

Direct Shear Test

In geotechnical engineering, this test is a commonly employed technique for determination of the shear strength of a soil. To determine the cohesiveness and internal friction angle, a soil sample is subjected to shearing forces in a controlled setting to determine the stability and bearing capacity of the soil, Additionally, determining the possible dangers related to foundation design, slope stability, and the overall performance of soil structures requires actual shear testing.by doing direct shear testing, engineers may assess how different loading situations affect the behavior of the soils and create safe and efficient construction methods.

Cohesion (c)

Cohesion is defined as the internal force that holds soil particles or molecules together. This characteristic is usually assessed in laboratory conditions through tests such as the direct shear test and the triaxial shear test. The Unconfined Compressive Strength (Suc) can also be evaluated using these techniques, and there are established relationships between Suc and shear strength, which can additionally be measured in the field through vane shear testing. In this investigation, soil cohesion was specifically assessed via the direct shear test.

Friction Angle (φ)

The friction angle indicates the capacity of soil or rock to withstand shear stress and is a vital factor in evaluating shear strength. It is typically determined in laboratory environments using either the direct shear test or the triaxial shear test. For granular soils, empirical correlations may also be applied to estimate this angle. In this study, the friction angle of the soil was determined using the direct shear test.

Figure 3.16: during preparation of a sample before loading(Reference Gondwana Engineering).

Figure 3.17: during loading(Reference Gondwana Engineering).

CHAPTER FOUR

4. Results and Discussions

4.1.Laboratory Test Results

Moisture Content

The moisture content was determined for three samples were brought to the laboratory during remolding a sample for Direct shear test and the values of the moisture content varies from 59.3% – 65.4%. The values of MC were very greater than the values mentioned by Das (2002) which is 30%-50% for clay soils consequently, the mass movement at Site 7 (104+140) was significantly influenced by elevated water content, particularly during the rainy season. The soil's water content in the research area increases with depth. Thus, as we delve deeper, the soil's water content becomes greater as we have seen in the table below.

Table 4.1: Moisture content

Sample name	Depth of sample taken (m)	Water content in %
Layer 1	0-1	59.3
Layer 2	1-5	63.7
Layer 3	5-10	65.4

Determination of Specific Gravity

The soil in the study area exhibits a specific gravity that ranges from 2.78 to 2.80. According to this test, the predominant soil types in the study area are clay and silty clay soils. This finding is consistent with the observations made by Das (2002), who noted that specific gravity values between 2.67 and 2.90 are characteristic of clay and silty clay soils. Furthermore, this test result encompasses the specific gravity of the study area. Consequently, the test suggests that the soil types present in the study area are clay and silty clay soils, which are generally weaker and possess multiple planes of weakness, thereby contributing to the occurrence of embankment failures at Site 7.

Table 4.2: Specific Gravity

Sample name	Sample depth (m)	The Average specific gravity
Layer 1	0-1	2.78
Layer 2	1-5	2.80
Layer 3	5-10	2.80

Unit Weight Determination

This examination is performed to evaluate the density of compacted in-situ soil. Nevertheless, a disturbed sample is collected and taken to the laboratory, where it is remolded to ascertain its unit weight. In the study area, the dry density and bulk density of the soils vary from 1.28 g/cm^3 to 1.42 g/cm^3 and from 2.04 g/cm^3 to 2.32 g/cm^3, respectively. As stated by Das (2002), silty sand soils are classified according to a dry unit weight that ranges from a minimum of 13 kN/m^3 to a maximum of 19 kN/m^3. The soils located at Site 7 (104+140) are identified as silty soils. Das also noted that soils with an avoid ratio ranging from a minimum of 0.4 to a maximum of 1, along with the dry unit weight, mostly apply to the soils found at Site 7 (104+140).

Table 4.3: Unit Weight

Sample name	Bulk Density (g/cm^3)	Unit Weight (Kn/m^3)	Dry Density (g/cm^3)	Dry Weight (Kn/m^3)
Layer 1	2.04	20.01	1.28	13
Layer 2	2.32	22.76	1.42	13.93
Layer 3	2.2	21.58	1.33	13.05

Grain Size Distribution

The distribution of grain sizes for soil samples collected from site 7 (104+140) indicates a combination of coarse and fine textures, particularly concerning the particles that are retained on the No. 4 sieve (4.75 mm) and those that pass through the No. 200 sieve (0.0075 mm). According to Table 4.4, the gravel content ranges from 3.1% to 4%, the sand content varies from 19.9% to 35.1%, and the clay content falls between 61.1% and 77%. It has been determined that the majority of the soil in this region is fine-grained, predominantly made up of silt and clay, indicating a high percentage of clay. This type of soil tends to swell when it gets wet and shrink when it dries out. As the surface area of these soil particles increases, their ability to hold water and swell also rises, which can weaken the soil's strength as moisture levels go up. These characteristics could be contributing to the slope instability observed at Site 7, particularly at station 104+140.

Table 4.4: Grain size Distribution

Sample name	Sample depth (m)	Percentage of Gravel	Percentage of Sandy Soil	Percentage of clay soil
Layer 1	0-1	3.3	35.1	61.1
Layer 2	1-5	4	20.4	75.6
Layer 3	5-10	3.1	19.9	77

Atterberg Limit

The findings of the soil masses' of Site 7 (104+140) were, liquid limit (LL), plastic limit (PL), and plastic index (PI) ranged from 60 to 65 percent, 29 to 32 percent, and 30 to 35 percent, respectively. The liquid limit (LL) of oven-dried samples from Site 7 varies between 60 and 65%, exceeding 50%. The plastic limit (PL) ranges from 29 to 32%, while the plasticity index (PI) is between 30 and 35%. The liquid index (LI) is observed to range from 0.08 to 0.28%. According to Skempton (1953), these values are consistent with those of clay soils, where LL ranges from 40 to 150%, PL from 30 to 50%, and PI from 15 to 100%. Terzaghi and Peck (1967) noted that the swelling characteristics of clay soils are indicated by the plasticity index, which shows a high swelling potential with values ranging from 20 to 55%. In this context, the swelling potential and PI of the soil in the study area at station 104+140 fall within the high swelling potential category. Furthermore, as stated by Wiley (2010), the LI value for the study area is also within the range of 0<LI<1, which characterizes the state and strength of fine-grained soil as being in a plastic state, exhibiting intermediate strength, and deforming similarly to a plastic material.

Table 4.5: Summary of Atterberg Limits

Sample name	sample depth (m)	LL (%)	PL (%)	PI (%)
Layer 1	0-1	65	32	33
Layer 2	1-5	64	29	35
Layer 3	5-10	60	30	30

4.2.Stability Analysis for Site 7 (104+140) LHS

The main goal here is to determine the minimum factor of safety (FS) and pinpoint where the critical slip surface is located. The model is created using Geo – Studio SLOPE/W, which examines two different scenarios for the placement of the piezometric line.

Case 1: When the Soil is fully saturated

This condition is conservative and it accounts for the worst-case scenario. This implies that the worst case applies during heavy rainfall or flooding condition.

Morgenstern-Price, Bishope and Janbu methods focus on fully saturated conditions. Steps to set up the model using Geo – Studio SLOPE/W and FS were found are:

Using Morgenstern–Price method

1.Defining the Geometry of the model by importing the DXF file of the AutoCAD drawing of the template and the Geometry have a side slope of 1.5:1 and a height of 10m and a width of 36m.

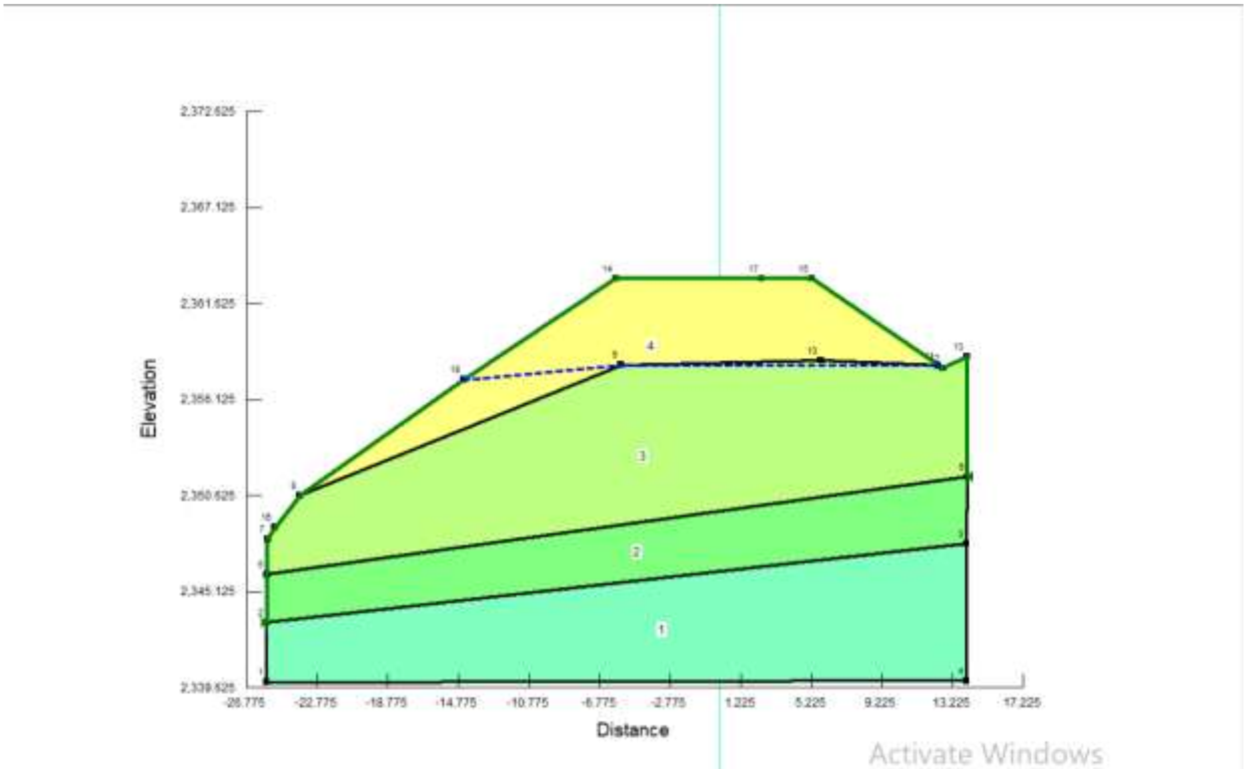

Figure 4.1: Defined Geometry, Material and Piezometric line

2. Defining the Material in the slope stability analysis using Mohr-Coulomb which uses the Shear strength parameters like Cohesion, Internal friction and the Unit weight of the soil mass and the materials are defined based on the Boreholes results.

3. Defining the Piezometric line for different conditions. The first is when the piezometric line is for fully saturated condition which is the worst-case scenario applies during heavy rainfall or flooding condition and the second condition is when the Piezometric line is at the toe of embankment.

4. Drawing a Slip surface is essential step to get a minimum safety factor in Geostudio/ Slop W software. In this model, the slip surface is characterized by utilizing the grid and radius options, resulting in the depiction of multiple slip surfaces for various radii.

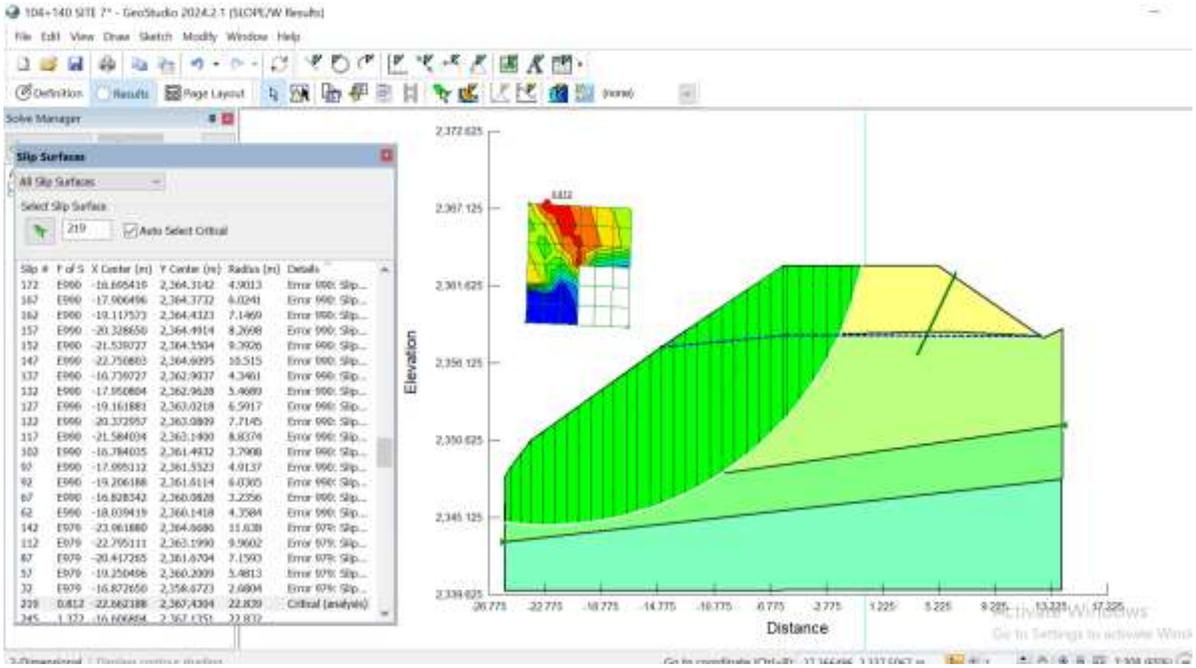

Figure 4.2: Critical Slip Surface using M-PM method

5.Generating a Mesh after drawing the slip surface, then running the software and a number of triangulations are formed for defined numbers this triangulations are called meshs.after meshing the factor of safety are computed.

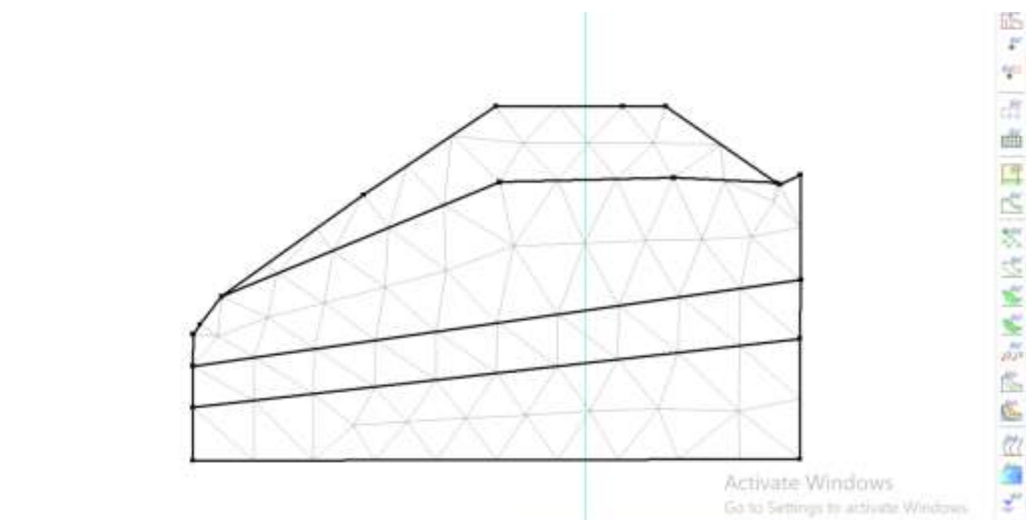

Figure 4.3: Meshing during running a software

6. The calculation of the factor of safety following the meshing process has been completed, and the factors of safety have been determined using various methods.

7. Draw Lambda Graph Vs Factor of Safety

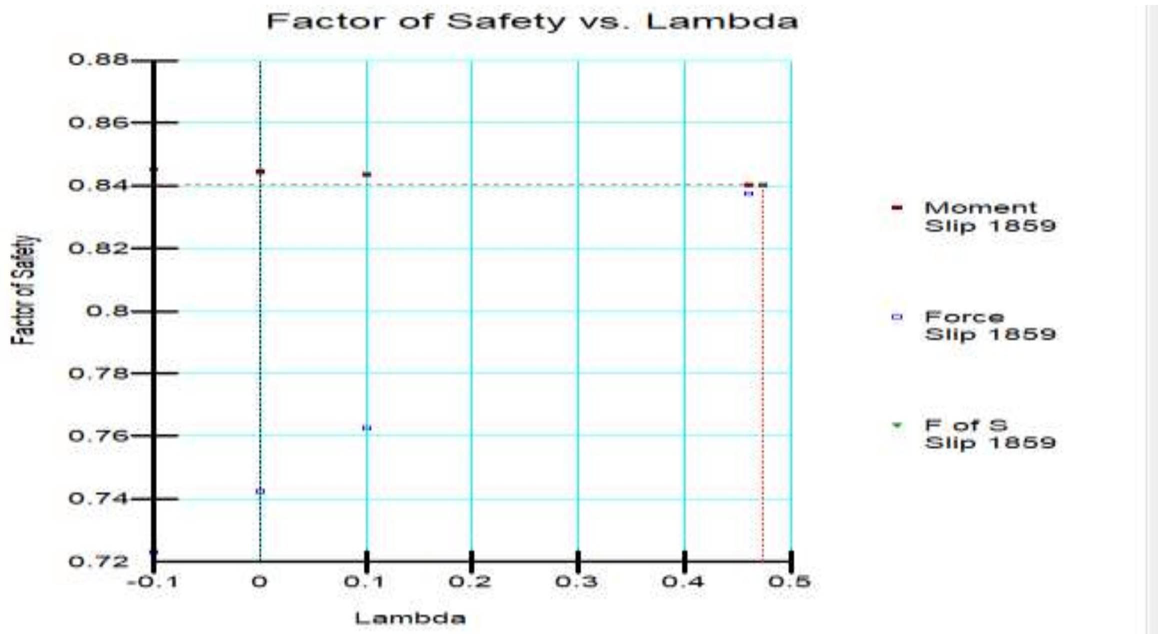

Figure 4.4: Lambda Graph Vs Factor of Safety

8. Draw a Force Polygon and Free body diagram

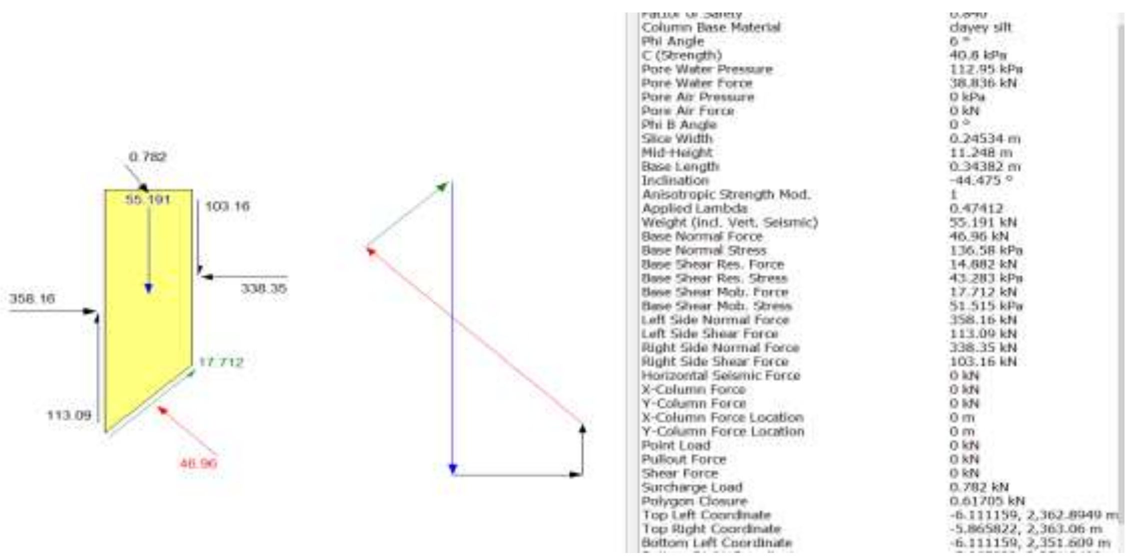

Figure 4.5: Force Polygon and Free body diagram

Case 2: When the Piezometer line is at the toe of the Embankment

Using Morgenstern–Price method

1.Defining the Geometry of the model by importing the DXF file of the AutoCAD drawing of the template and the Geometry have a side slope of 1.5:1 and a height of 10m and a width of 36m.

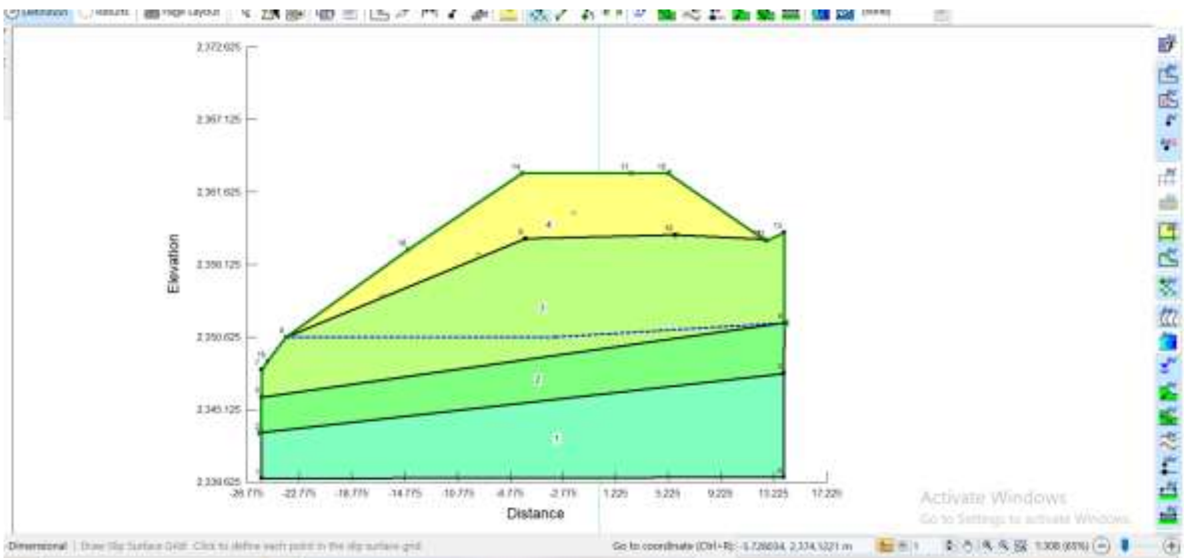

Figure 4.6: Defined Geometry, Material and Piezometric line

2. Defining the Material in the slope stability analysis using Mohr-Coulomb which uses the Shear strength parameters like Cohesion, Internal friction and the Unit weight of the soil mass and the materials are defined based on the Boreholes results.

3. Defining the Piezometric line for different conditions. The first is when the piezometric line is for fully saturated condition which is the worst-case scenario applies during heavy rainfall or flooding condition and the second condition is when the Piezometric line is at the toe of embankment.

4. Drawing a Slip surface is essential step to get a minimum safety factor in Geostudio/ Slop W software. In this model the slip surface is defined using grid and radius option a number of slip surfaces are drawn for different radii.

5. Generate Slip Surfaces

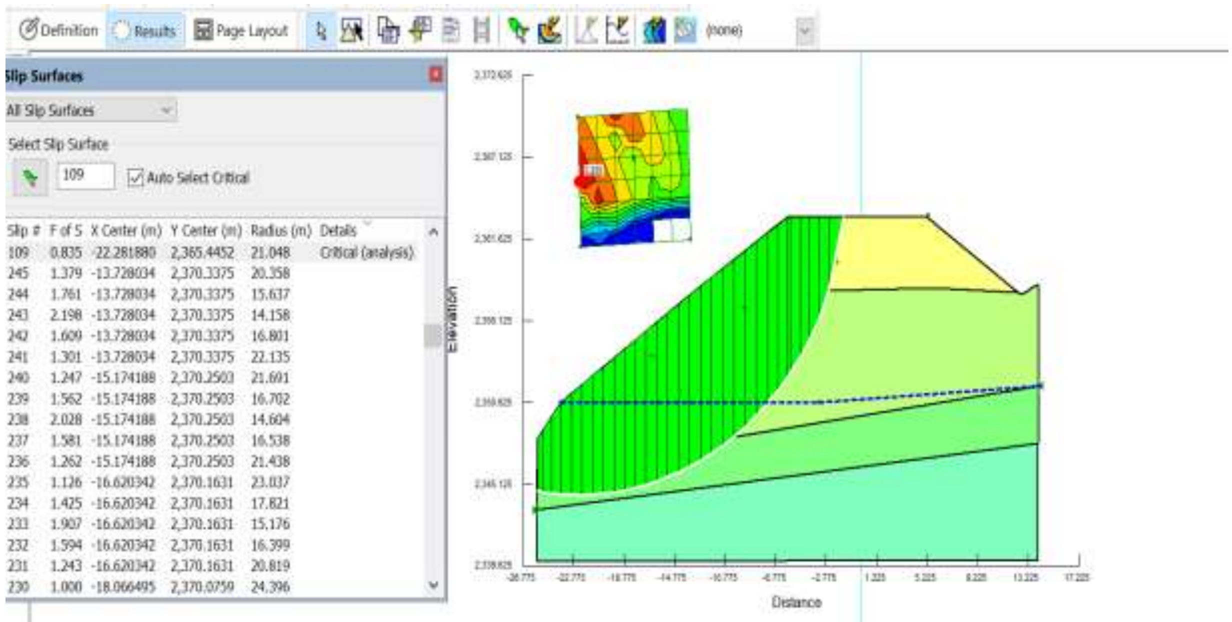

Figure 4.7: Critical Slip Surface using M-PM method

6.Generating a Mesh after drawing the slip surface, then running the software and a number of triangulations are formed for defined numbers this triangulations are called meshs.after meshing the factor of safety are computed.

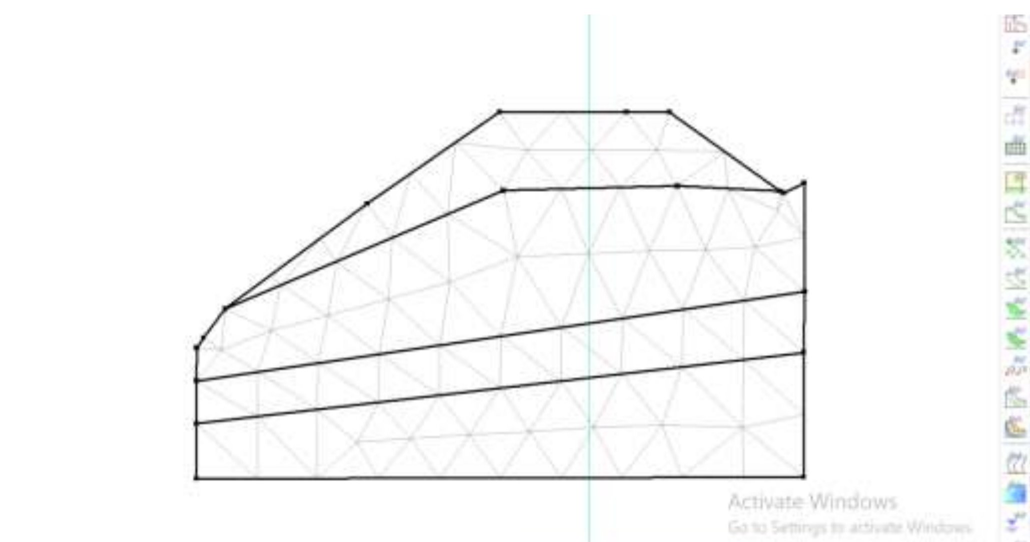

Figure 4.8: Meshing during running a software

7. Draw Lambda Graph Vs Factor of Safety

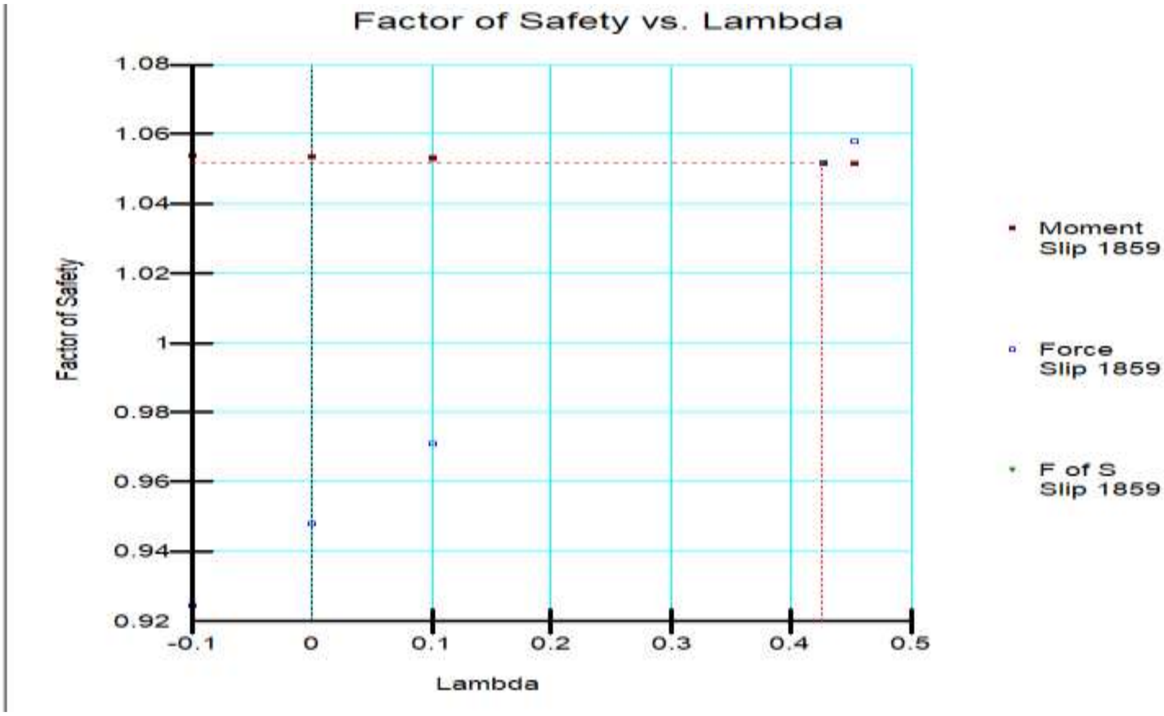

Figure 4.9: Lambda Graph Vs Factor of Safety

8. Draw a Force Polygon and Free body diagram

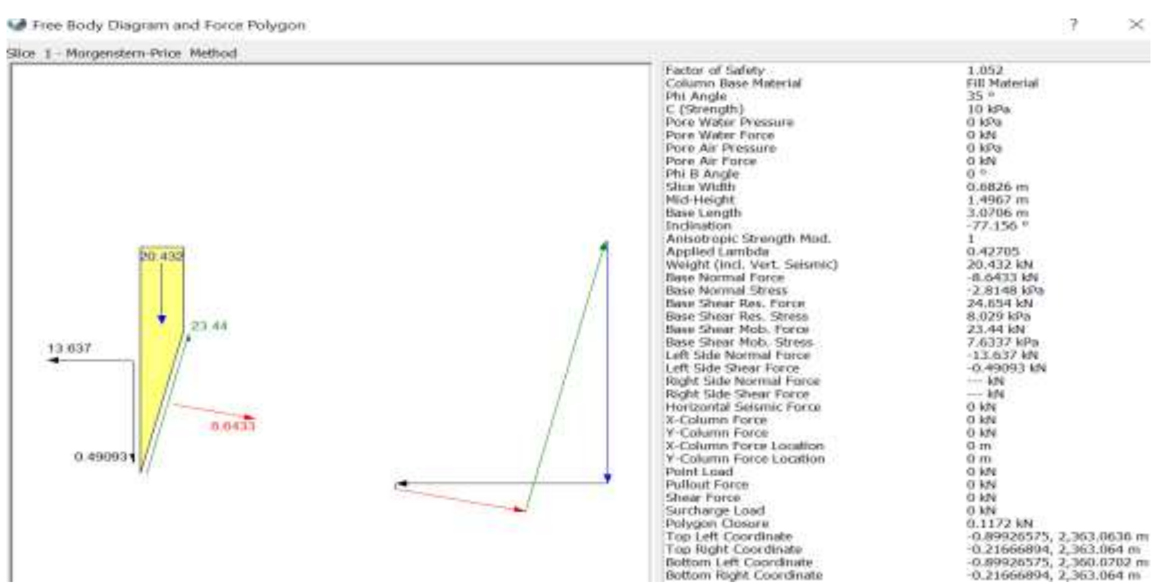

Figure 4.10: Force Polygon and Free body diagram

Table 4.6: Summary of Minimum Factor of safety for Site 7 (104+140) Embankment section

Slope Section	Methods	Factor of Safety		Slope Status
		Ground water conditions		
		Fully Saturated	at the Toe	
Section 7	Morgenstern–Price	0.812	0.835	Un stable
	Bishop	0.727	0.863	Un stable
	Janbu	0.729	0.755	Un stable

4.3.Seismic

In Ethiopia, seismic zones are classified using the Ethiopian Building Code Standard (CES-8:2015).According to this criteria, Ethiopia is categorized into four seismic zones.

- Zone 0: Represents regions characterized by minimal seismic activity
- Zone 1: Signifies areas of low seismicity
- Zone 2: Encompasses regions with moderate levels of seismic activity
- Zone 3: Identifies areas that experience significant seismicity

The seismic zone of the study area is belongs to Zone 0: Very low seismicity, seismicity has not been considered in the slope stability analysis.

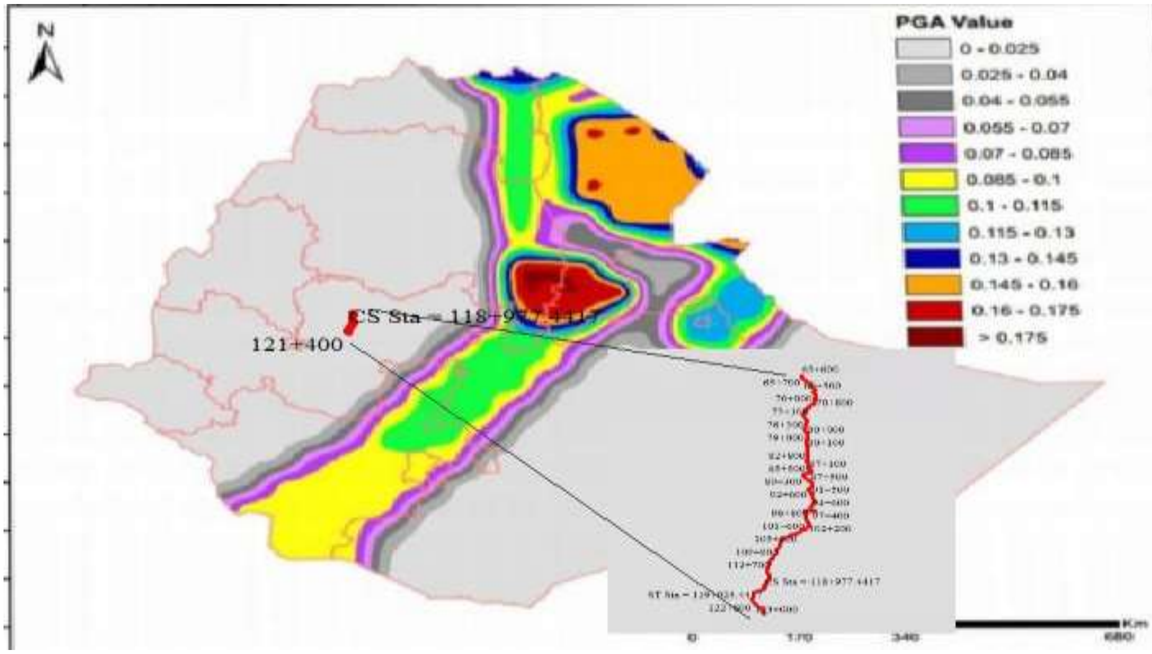

Figure 4.11: Seismic map of the study area

4.4. Causes and Triggering Factors of Embankement failures in Bako-Shambu road project

Based on the results obtained from laboratory tests, field observations, and software analyses, the following factors are identified as triggers for landslides in the study area.

Type of Soil

The test results indicate that the soils in the study area consist of clay soil. This type of soil is recognized for its tendency to expand when saturated and contract during dry conditions, often exhibiting several planes of weakness that can trigger landslides in the Bako-Shambu road project area. Therefore, the soil type present in the study area was responsible for the landslide that occurred in this region.

Steep Slope

All failed sites are situated in the gently-moderately sloping hills related to embankment failures and side slope failures. Thus the landslide has occurred in gentle to very gentle slope gradient. The steeper slope gradient of the study area also caused the occurrence of rock fall, debris, and earthflow besides, the slope gradient, the orientation, and the shape of the slope also have a great effect on slope stability problems in the study area.

Geological Factors

Geophysical survey identified three formations in all sites that are classified as top soil unit, intermediate unit (decomposed and highly weathered section representing the top section of the bed rock) and the bed rock having low water absorption. Thus due do those weak layers, leads to the instability of the study area.

Ground water

Groundwater conditions can really differ from one location to another, thanks to the types of rocks and the lay of the land. Typically, groundwater shows up as seepage on sloped areas and at lower elevations where the ground is flatter. The saturation levels and the depth of the aquifer can also change quite a bit. When the rainy season hits, the volume of groundwater tends to rise, which can lead to a thinner unsaturated zone. This thinning of the unsaturated zone can, in turn, increase the risk of slope instability.

Rainfall

Rain-induced slope instability is a common geotechnical issue. One of the main causes behind landslides in regions with significant annual rainfall is, predictably, the rain itself. Over time, extensive and heavy rainfall—particularly during the two monsoon seasons each year—can infiltrate into slopes and result in saturation at shallow depths (Idrus et al., 2023). For the Bako-Shambu road project, the average annual rainfall over the past decade has ranged from 1100mm to 1450mm, with specific years seeing totals between 1000mm and 1200mm. The highest rainfall recorded in Bako was in 2017, while Shambu saw its peaks in 2015 and 2020. The rainy season, primarily from June to September, brings the heaviest downpours, which further saturate the soil and reduce its shear strength, ultimately triggering landslides in the area. Thus, rainfall is a key factor to consider when assessing landslide risks in this region.

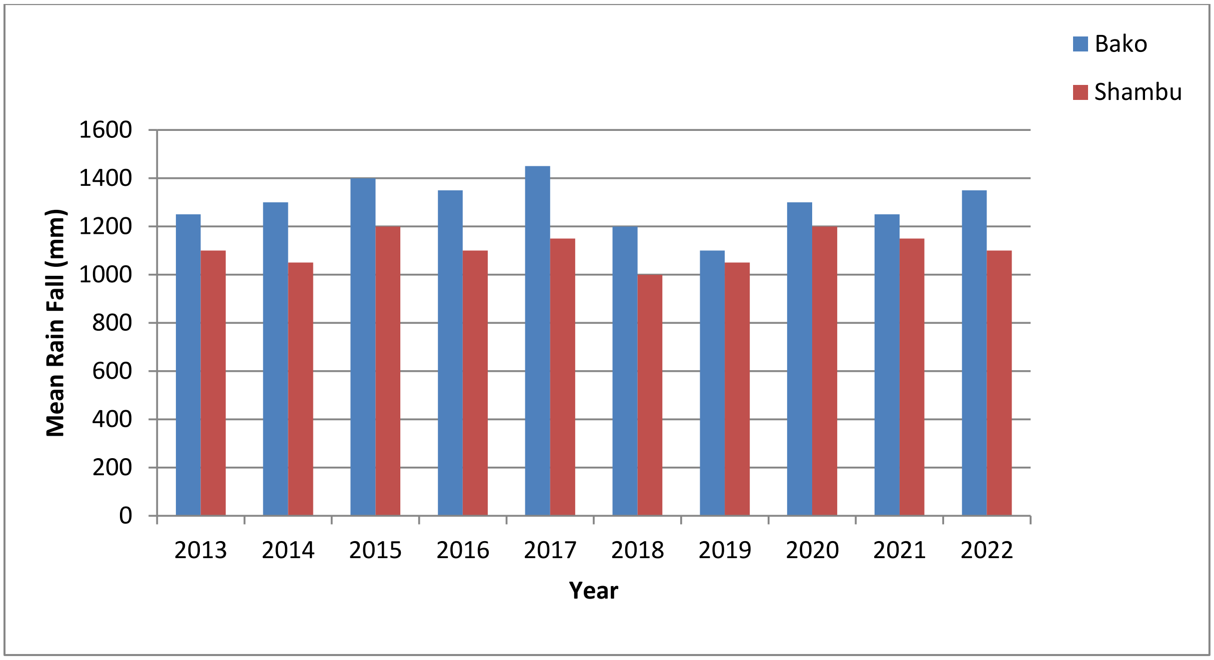

Figure 4.12: Annual rainfalls Analysis of Bako and Shambu Towns

CHAPTER FIVE

5. Conclusion and Recommendations

5.1.Conclusions

During site investigation visual identified of the formations soils in all sites that are classified as top soil unit (residual soil, colluvial and alluvial deposit), intermediate unit (decomposed and highly weathered section representing the top section of the bed rock) and the bed rock having low water absorption. Thus due do those weak layers, leads to the instability of the study area.

According to the results of the laboratory tests, the Atterberg limit indicates that the soil is classified as clay, exhibiting high plasticity and significant swelling potential, making it sensitive to moisture that can trigger sliding. The grain size analysis reveals that over 71% of the soil types are primarily composed of fine-grained soils, which possess high plastic clay characteristics and are easily influenced during saturation, thereby contributing to instability in the study area. The specific gravity measurement for the study area suggests that the soil falls within the specific gravity range typical of clay and silty clay soils, which possess multiple planes of weakness that can lead to slope instability.

The analysis of slope stability was conducted utilizing Geostudio/SlopW software for different cases the first one is when the water table is fully saturated which is the worst se scenario. This implies that the worst case applies during heavy rainfall or flooding condition and the FS is decreased for different methods. For the second case when the water table is at the toe of the embankment, the value of FS in increasing. Consequently, this indicates that the rainfall recorded in the study area was one of the primary factors that triggered the landslide.

5.2. Recommendations

For these sites (Site-1 (94+160 to 94+210), Site-3 (97+800 to 97+880),Site-5 (96+660 to 96+690),Site-7 (104+050 to 104+230) and Site-11 (98+280-98+370) The cause of failures is that they are constructed on thick, soft and wet residual formation that can be unstable by surface and subsurface water flow and nearby river saturation and erosion. Therefore provide protection works like: Gabion box, retaining wall, side ditch, culverts and cross-drain.

For these sites (Site-1 (94+160 to 94+210), Site-3 (97+800 to 97+880),Site-5 (96+660 to 96+690),Site-7 (104+050 to 104+230) and Site-11 (98+280-98+370) Provide pavement protection works like: excavate the full section of the subgrade layer for 60cm and replace with a rock fil and compact as required, A geo-grid or geotextile, as appropriate, to be placed on top of the levelled rock fills, before carrying out the next steps of the embankment construction. Then continue the next layers as per the original design up to the subbase level to improve stability.

<u>Site 7</u>

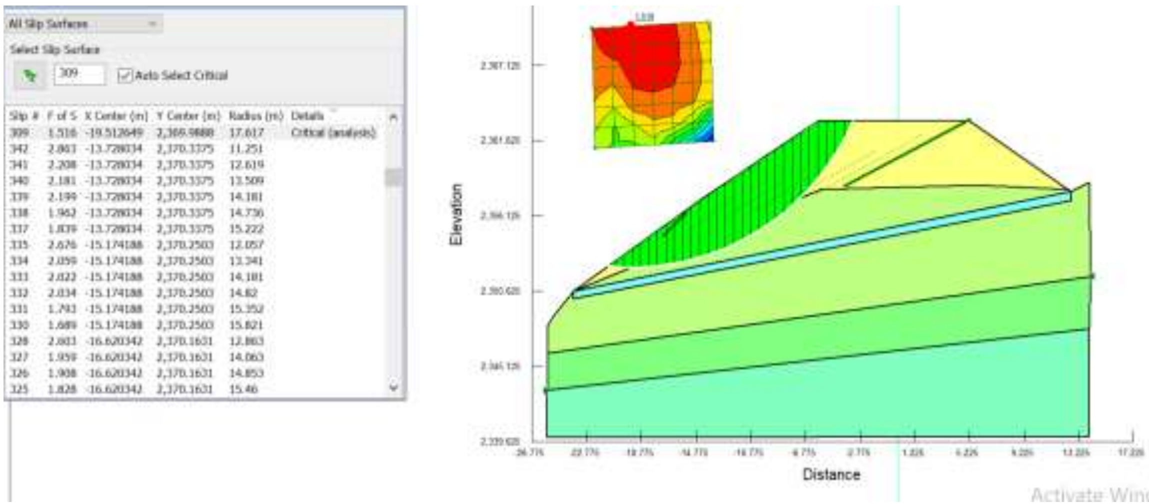

Figure 4.12: FS after excavating the subgrade and replacing with 60cm Rock fill for site 7

For these sites Site-6 (km 99+800 to km 99+920) and Site-7 (104+050 to 104+230) realign the road to avoid the construction of the fill section in water logged colluvium material area.

REFERENCES

1. Wang, G. and Sassa, K. (2003) ‘Pore-pressure generation and movement of rainfallinduced landslides: Effects of grain size and fine-particle content’, Engineering Geology, 69(1–2), pp. 109–125. doi: 10.1016/S0013-7952(02)00268-5.

2.Adane´s “Investigation on causes of Landslide in the Blue Nile Basin Gohatsion-Dejen Road As case study”, Thesis for Master Of Science Degree, Addis Ababa University,2012

3. Jaspreet Singh1, Dilan Robert1? Peihan Wang1, Filippo Giustozzi1, Mojtaba Mahmoodian1, Sujeeva Setunge1 and Brian O’Donnell2 (2017)" Stability assessment of enzyme stabilized road embankments."

4. Asmelash Abay Hagos., (2012). Remote Sensing & GIS-based Mapping on Landslide Phenomena& Landslide Susceptibility Evaluation of Debresina area (Ethiopia) & R.S. Girolamo basin (Sardinia).Università Degli Studi di Cagliari: Ph.D. thesis.

5. Krishna Prasad Aryal (2006) "Slope Stability Evaluations by Limit Equilibrium and Finite Element Methods."

6. Tekalgn, (2016). Investigation of slope failure problems along Arbaminch-Gidole road as a casestudy, MSc. Thesis, Addis Ababa University

7. Hammouri, N. A., Malkawi, A. I. H., Yamin, M. M. J. B. o. E. G., & Environment, t. . (2008). Stability analysis of slopes using the finite element method and limiting equilibrium approach. 67,471-478

8. Rajabi, A. M. (2021). Earthquake-induced landslide prediction using Earthquake-induced landslide prediction using Earthquake-induced landslide prediction using. under exclusive licence to Springer Nature B.V. 2021 https://doi.org/10.1007/s11069-021-04963-8

9. Zhang, W., Gu, X., Han, L., Wu, J., Xiao, Z., Liu, M., & Wang, L. . (2022). Zhang, W., Gu, X.,Han,L. A short review of probabilistic slope stability analysis considering spatial variability of geomaterial parameters. . Zhang, W., Gu, X., Han, L., Wu, J., Xiao, Z., Liu, M., & Wang, L. (2022). A short review of probabilistic slope stabili Innovative Infrastructure Solutions, , 7(7),249

10. Nandhini. S., Seyamala. S. (2020) "Investigation studies on embankment failure”

11. Ullah et al. (2020), “Brief Review of Slope Stability Analysis Methods”

12. Fisseha, S. and Mewa, G. (2016) ‘Road failure caused by landslide in north Ethiopia: A case study from Dedebit - Adi-Remets road segment’, Journal of African Earth Sciences, 118, pp. 65–74. doi: 10.1016/j.jafrearsci.2016.02.022

13. A.Burman, S.Acharya, R.sahayetal. (2015) “A comparative study of slope stability analysis using traditional limit equilibrium method and finite element method.”

14.Juliana Idrus , Norhanizah Hamzah, Rozaini Ramli, Masyitah Md Nujid & Siti Fatimah 15.Sadikon(2023) “Enhancing Slope Stability with Different Slope Stabilization Measures: A Case Study using SLOPE/W Software”

16. R. Desai & R. Joshi, (2019). “Slope stability evaluations by limit equilibrium and finite element method.”

17. Panda & Behera, (2021) "Slope Stability Analysis Lampung using Computational Analysis Program"

18. Komolvial, ,. V. (2021). Failure analysis on a heavy rainfall-induced landslide in Huay Khab Failure analysis on a heavy rainfall-induced landslide in Huay Khab. *Science Press, Institute of Mountain Hazards and Environment, CAS and Springer-Verlag GmbH Germany, part of Springer Nature*.

19. Fisseha, S., & Mewa, G, (2016). “Road failure caused by landslide in north Ethiopia: A case study from Dedebit–Adi-Remets road segment.” Journal of African Earth Sciences, 118, 65-74.

20. (Wendim ET al.2023). “Causes, Failure Mechanisms and Susceptibility Zonation of Landslides along Gedo-Dilb Road Corridor, Northern Ethiopian.”

21. (Kifle Weldearegay, 2013). “Review of the occurrences and influencing factors of landslides in the highlands of Ethiopia: With implications for infrastructural development.”

22. (Che Mamat ET al.2022). “Slope Stability Prediction of Road Embankment using Artificial Neural Network Combined with Genetic Algorithm.”R. (Anggiawan et al 2025). “Slope stability analysis due to water level change of the Dadahup-G1/A5-B4 Road embankment.”IOP Conf. Ser.: Earth Environ. Sci. 1488 012046

APPENDICES

Appendix A: Laboratory Tests

A.1 Atterberg limit

Table A.1.1 Atterberg Limits at 104+140 (Layer 1)

Liquid limit Determination					***Plastic Limit***		
Number of Blows	28	23	18		1	2	3
Can no.	A1	A2	A3		37.5	35.21	29.36
Wet Weight + Tare, gm	39.9	45.8	38.7		35.13	33.48	26.01
Dry Weight + Tare, gm	31.2	34.9	30.2		26	25.42	17.2
Weight of Tare, gm	17.5	18.1	17.6		2.37	2.52	3.35
Weight of Water, gm	8.7	10.9	8.3		9.13	8.06	8.81
Dry Weight , gm	13.6	16.8	12.6		26.0	31.27	38.02
Moisture Content %	63.9	65.0	66.1	**65**	**32**		

Liquid limit	**65**
Plastic limit	**32**
Plasticity index	**33**

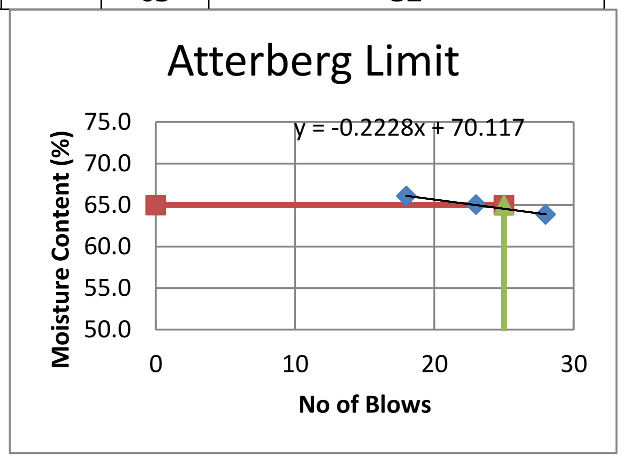

Table A.1.2 Atterberg Limits at 104+140 (Layer 2)

Liquid limit Determination					***Plastic Limit***		
Number of Blows	30	25	22		4	5	6
Can no.	B1	B2	B3		28.1	27.5	28.1
Wet Weight + Tare, gm	48.8	53.2	46.3		25.8	24.9	25.2
Dry Weight + Tare, gm	36.9	39.1	34.6		16.2	16.2	16.5
Weight of Tare, gm	17.7	17.8	17.4		2.4	2.6	2.9
Weight of Water, gm	11.8	14.1	11.7		9.6	8.7	8.7
Dry Weight , gm	18	21.4	17.3		24.5	29.59	33.53
Moisture Content %	60	64	67.7	**29**			

Liquid limit	**64**
Plastic limit	**29**
Plasticity index	**35**

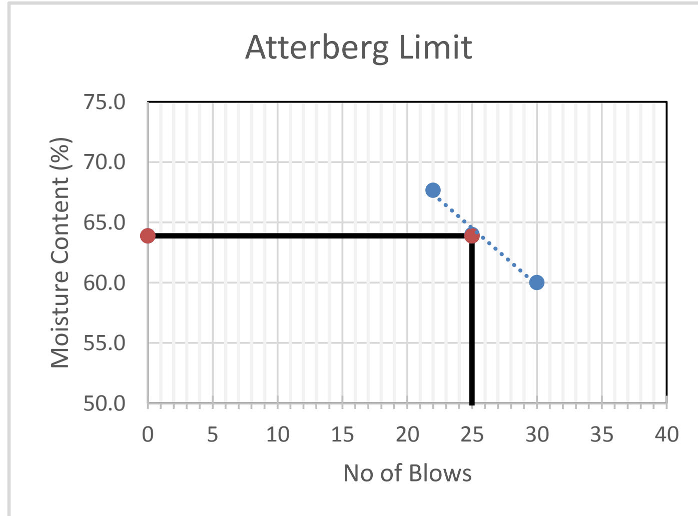

Table A.1.3 Atterberg Limits at 104+140 (Layer 3)

Liquid limit Determination					***Plastic Limit***		
Number of Blows	20	25	28		7	8	9
Can no.	C1	C2	C3		37.5	37.7	36.37
Wet Weight + Tare, gm	39.9	45.8	38.7		35.1	35.21	33.37
Dry Weight + Tare, gm	31.2	34.9	30.2		26.44	26.8	26.46
Weight of Tare, gm	17.5	18.1	17.6		2.4	2.49	2.6
Weight of Water, gm	8.7	9.0	8.3		9	8.41	6.91
Dry Weight , gm	13.6	16.8	12.6		29.0	29.61	30.00
Moisture Content %	60.5	60.3	58.0	**60**	**30**		

Liquid limit	**60**
Plastic limit	**30**
Plasticity index	**30**

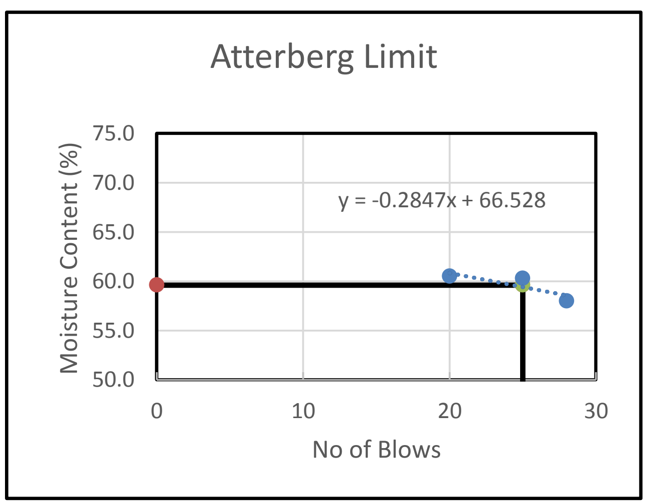

A.2 Moisture Content

Table A.2.1 Moisture Content at 104+140 (Layer 1)

MOISTURE CONTENT (Layer 1)			
Location	26+250	*Pit No*	
Source	Bako	*Mat. Classification*	A-7
Date of Sampling	14 March 2024	*Sampled for*	Thesis
Date Of Testing	18 April 2024	*Depth*	0-1
Moisture Content			
Depth of Sample		1m	1m
Container No		100 kpa	200 kpa
Wt of Container + Wet Soil		202	201
Wt of Container + Dryt Soil		133.6	132.3
Wt of Water (gm)		68.4	68.7
Wt. of Cont.(gm)		25.6	25.3
Wt of Dry Soil (gm)		104.65	105.0
Moisture Content (%)		65.4	65.4
Average Moisture Content (%)		65.4	

Table A.2.2 Moisture Content at 104+140 (Layer 2)

MOISTURE CONTENT (Layer 2)			
Location	26+250	*Pit No*	
Source	Bako	*Mat. Classification*	A-7
Date of Sampling	14 March 2024	*Sampled for*	Thesis
Date Of Testing	18 April 2024	*Depth*	1−5
Moisture Content			
Depth of Sample		1m	1m
Container No		100 kpa	200 kpa
Wt of Container + Wet Soil		201.22	201.63
Wt. of Container + Dry Soil		132.09	133.77
Wt. of Water (gm)		69.13	67.86
Wt. of Cont.(gm)		25.6	25.3
Wt. of Dry Soil (gm)		108	107.0
Moisture Content (%)		64.0	63.4
Average Moisture Content (%)		63.7	

Table A.2.3 Moisture Content at 104+140 (Layer 3)

ATTERBERG LIMITS (AASHTO T90)			
Location	26+250	*Pit No*	
Source	Bako	*Mat. Classification*	A-7
Date of Sampling	14 March 2024	*Sampled for*	Thesis
Date Of Testing	18 April 2024	*Depth*	5−10
Moisture Content			
Depth of Sample		1m	1m
Container No		100 kpa	200 kpa
Wt. of Container + Wet Soil		200.5	201
Wt. of Container + Dry Soil		135	136
Wt. of Water (gm)		65.5	65
Wt. of Cont.(gm)		25.6	25.3
Wt. of Dry Soil (gm)		109.4	110.7
Moisture Content (%)		59.9	58.7
Average Moisture Content (%)		**59.3**	

A.3 Sieve Analysis

Table A.3.1 Grain Size Distribution Analysis at 104+140 (Layer 1)

Sieve analysis for soil classification			
Wt. of sample before washing			500
Wt. of sample after washing			197
Washed out			303
Sieve Size	Wt. Ret.	% Ret.	% Pass
No10	16.6	3.3	**96.7**
No40	59.2	11.8	**84.8**
No.200	116.2	23.2	**61.6**
Pan	4.5	100.0	

Liquid limit	**65**
Plastic limit	**32**
Plasticity index	**33**
AASHTO Soil class.	**A-7-5(20)**

Table A.3.2 Grain Size Distribution Analysis at 104+140 (Layer 2)

Wt. of sample before washing			500
Wt. of sample after washing			197
Washed out			303
Sieve Size	Wt. Ret.	% Ret.	% Pass
No10	16.6	3.3	**96.7**
No40	59.2	11.8	**84.8**
No.200	116.2	23.2	**61.6**
Pan	4.5	100.0	

Liquid limit	**64**
Plastic limit	**29**
Plasticity index	**35**
AASHTO Soil class.	**A-7-5(20)**

Table A.3.3 Grain Size Distribution Analysis at 104+140 (Layer 2

Wt. of sample before washing			500
Wt. of sample after washing			197
Washed out			303
Sieve Size	Wt. Ret.	% Ret.	% Pass
No10	16.6	3.3	**96.7**
No40	59.2	11.8	**84.8**
No.200	116.2	23.2	**61.6**
Pan	4.5	100.0	

Liquid limit	**60**
Plastic limit	**30**
Plasticity index	**30**
AASHTO Soil class.	**A-7-5(20)**

A.4 Unit weight

Table A.4.1 Unit weight at 104+140 (Layer 1)

Trial No.	1	2	3
Weight of Mold + Wet soil (g)	335	334.6	334.9
Weight of Mold (g)	151.4	151.4	151.4
Weight of Wet soil (g)	183.6	183.2	183.5
Volume of Mold (cc)	90	90	90
Wet density (g / cm3)	2.04	2.04	2.04
Average Wet density (g / cm3)	**2.04**		

Moisture Content		
Container No		
Wt. of Container + Wet Soil	200.5	201
Wt. of Container + Dry Soil	135	136
Wt. of Water (gm)	65.5	66
Wt. of Cont.(gm)	25.6	25.3
Wt. of Dry Soil (gm)	109.4	110.7
Moisture Content (%)	59.9	59.6
Average Moisture Content (%)	**59.7**	
Dry Density (g / cm3)	1.28	1.28
Average Dry Density (g / cm3)	**1.28**	

Table A.4.2 Unit weight at 104+140 (Layer 2)

Trial No.	1	2	3
Weight of Mold + Wet soil (g)	335	334.6	334.9
Weight of Mold (g)	151.4	151.4	151.4
Weight of Wet soil (g)	194.8	196.9	201.0
Volume of Mold (cc)	90	90	90
Wet density (g / cm3)	2.16	2.19	2.23
Average Wet density (g / cm3)	**2.20**		
Moisture Content			
Container No			
Wt. of Container + Wet Soil	202	201	
Wt. of Container + Dry Soil	133.6	132.3	
Wt. of Water (gm)	68.4	68.7	
Wt. of Cont.(gm)	25.6	25.3	
Wt. of Dry Soil (gm)	104.65	105.0	
Moisture Content (%)	65.4	65.4	
Average Moisture Content (%)	**65.4**		
Dry Density (g / cm3)	1.33	1.33	
Average Dry Density (g / cm3)	**1.33**		

Table A.4.3 Unit weight at 104+140 (Layer 3)

Trial No.	1	2	3
Weight of Mold + Wet soil (g)	335	334.6	334.9
Weight of Mold (g)	151.4	151.4	151.4
Weight of Wet soil (g)	198.9	211.5	216.9
Volume of Mold (cc)	90	90	90
Wet density (g / cm3)	2.21	2.35	2.41
Average Wet density (g / cm3)	**2.32**		
Moisture Content			
Container No			
Wt. of Container + Wet Soil	201.22	201.63	
Wt. of Container + Dry Soil	132.09	133.77	
Wt. of Water (gm)	69.13	67.86	
Wt. of Cont.(gm)	25.6	25.3	
Wt. of Dry Soil (gm)	108	107.0	
Moisture Content (%)	64.0	63.4	
Average Moisture Content (%)	**63.7**		
Dry Density (g / cm3)	1.42	1.42	
Average Dry Density (g / cm3)	**1.42**		

A.5 Specific Gravity

Table A.5.1 Specific Gravity at 104+140

Sample name	Layer 1			Layer 2			Layer 3		
Depth (m)	0-1			1−5			5−10		
Trial No.	1	2	3	1	2	3	1	2	3
Code	1	2	3	A	B	C	A	B	C
Mass of empty pycnometer, Wp (g)	28.56	28.41	27.66	27.95	28.31	28.68	27.95	28.31	28.68
Mass of pycnometer+ dry soil (g), Wps	38.51	38.44	37.72	37.94	38.14	38.84	37.94	38.24	38.84
Mass of dry soil (g)	9.95	10.03	10.06	9.99	9.83	10.16	9.97	9.93	10.11
Mass of pycnometer + dry soil + water (g), Wpsw	86.17	85.94	84.59	84.45	85.52	85.01	84.45	85.52	85.01
Mass of pycnometer + water (g), Wpw	79.9	79.4	78.17	78.17	79.4	78.17	78.17	79.4	78.17
Specific gravity, Gs	2.70	2.87	2.76	2.69	2.65	3.06	2.70	2.61	3.09
Average Specific gravity, Gs	2.78			2.80			2.80		

Appendix B: Slope Stability Analysis Results Using Geostudio software

Using Bishop Method

Case 1: When the Soil is fully saturated

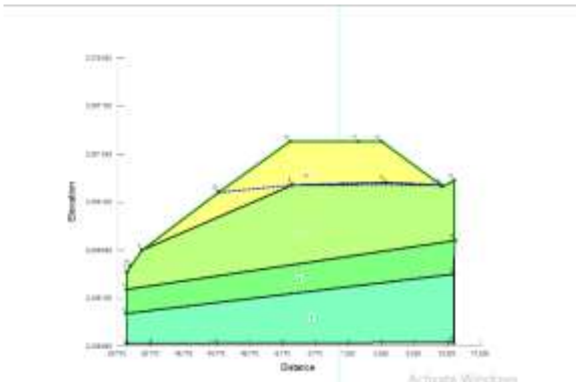

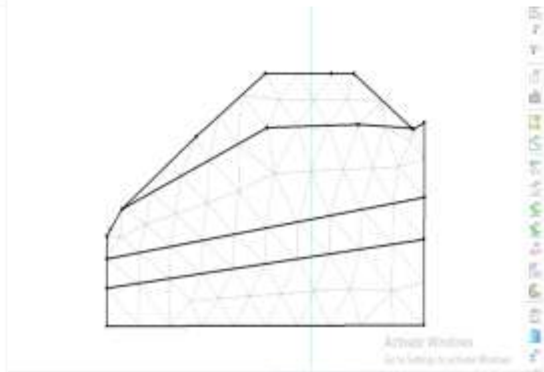

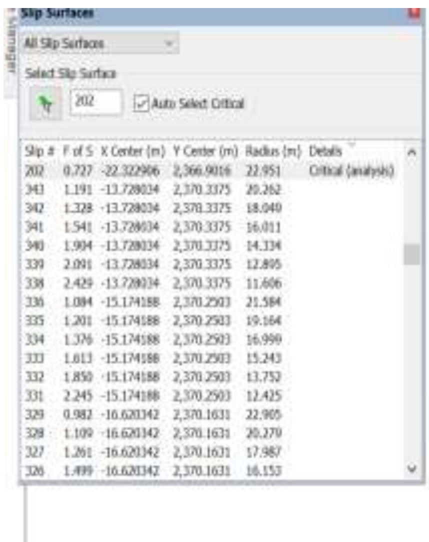
Slip Surfaces

All Slip Surfaces

Select Slip Surface

202 ☑ Auto Select Critical

Slip #	F of S	X Center (m)	Y Center (m)	Radius (m)	Details
202	0.727	-22.322906	2,366.9016	22.951	Critical (analysis)
343	1.191	-13.728034	2,370.3375	20.262	
342	1.328	-13.728034	2,370.3375	18.049	
341	1.541	-13.728034	2,370.3375	16.011	
340	1.904	-13.728034	2,370.3375	14.334	
339	2.091	-13.728034	2,370.3375	12.895	
338	2.429	-13.728034	2,370.3375	11.606	
336	1.084	-15.174188	2,370.2503	21.584	
335	1.201	-15.174188	2,370.2503	19.164	
334	1.376	-15.174188	2,370.2503	16.999	
333	1.613	-15.174188	2,370.2503	15.243	
332	1.850	-15.174188	2,370.2503	13.752	
331	2.245	-15.174188	2,370.2503	12.425	
329	0.982	-16.620342	2,370.1631	22.905	
328	1.109	-16.620342	2,370.1631	20.279	
327	1.261	-16.620342	2,370.1631	17.987	
326	1.499	-16.620342	2,370.1631	16.153	

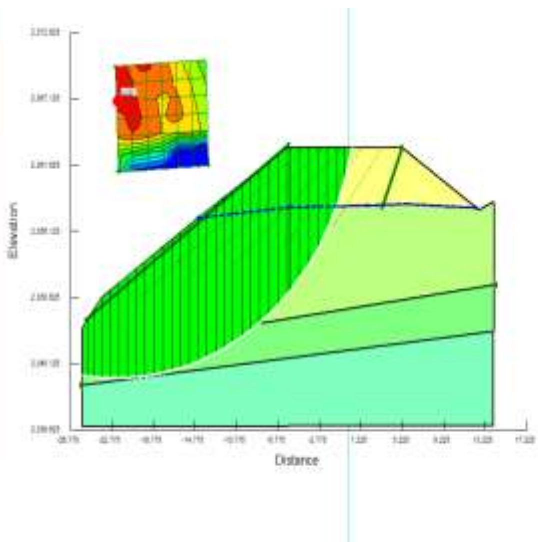

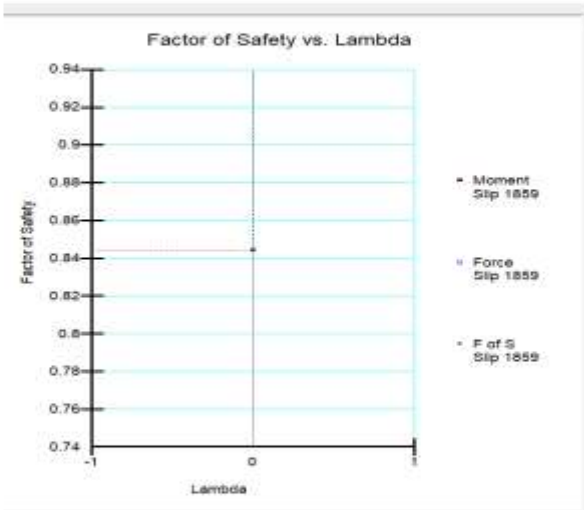

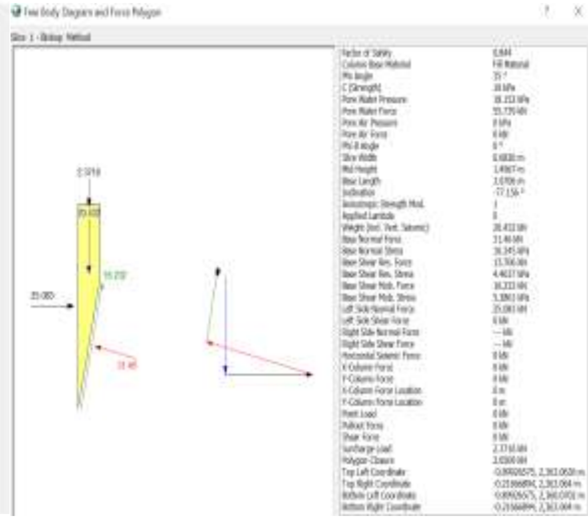

Case 2: When the Piezometric line is at the toe of the Embankment

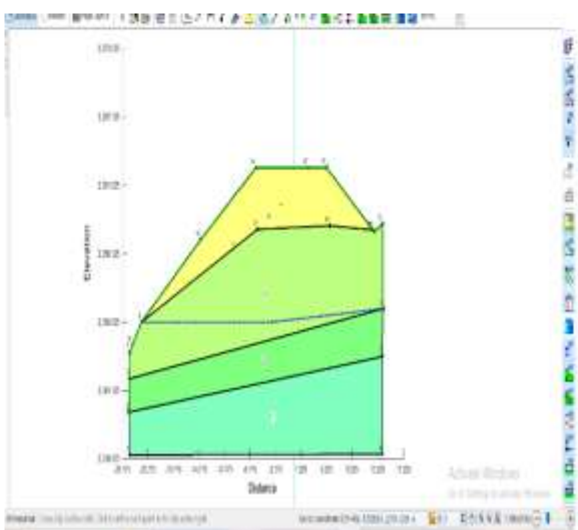
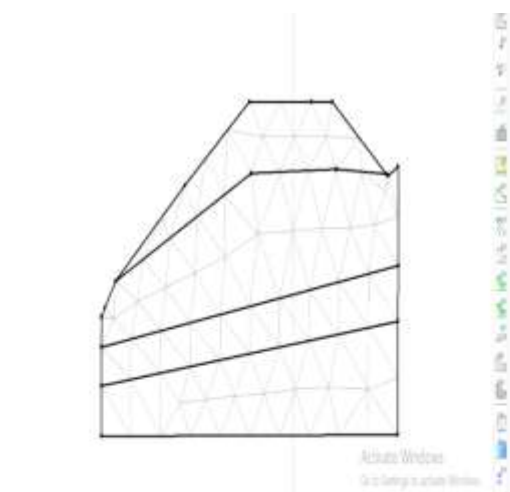

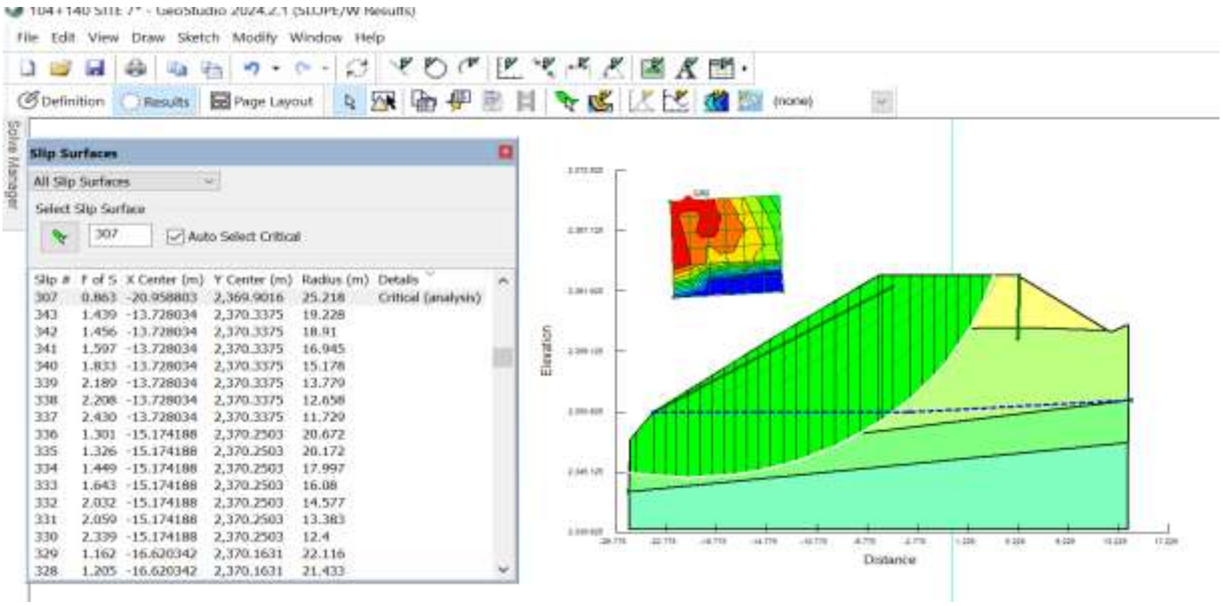
File Edit View Draw Sketch Modify Window Help
Definition
Results
Page Layout
(none)
Solve Manager
Slip Surfaces
All Slip Surfaces
Select Slip Surface
307
Auto Select Critical
Slip # F of S X Center (m) Y Center (m) Radius (m) Details
307 0.863 -20.958803 2,369.9016 25.218 Critical (analysis)
343 1.439 -13.728034 2,370.3375 19.228
342 1.456 -13.728034 2,370.3375 18.91
341 1.597 -13.728034 2,370.3375 16.945
340 1.833 -13.728034 2,370.3375 15.178
339 2.189 -13.728034 2,370.3375 13.779
338 2.208 -13.728034 2,370.3375 12.658
337 2.430 -13.728034 2,370.3375 11.729
336 1.301 -15.174188 2,370.2503 20.672
335 1.326 -15.174188 2,370.2503 20.172
334 1.449 -15.174188 2,370.2503 17.997
333 1.643 -15.174188 2,370.2503 16.08
332 2.032 -15.174188 2,370.2503 14.577
331 2.059 -15.174188 2,370.2503 13.383
330 2.339 -15.174188 2,370.2503 12.4
329 1.162 -16.620342 2,370.1631 22.116
328 1.205 -16.620342 2,370.1631 21.433
Elevation
Distance

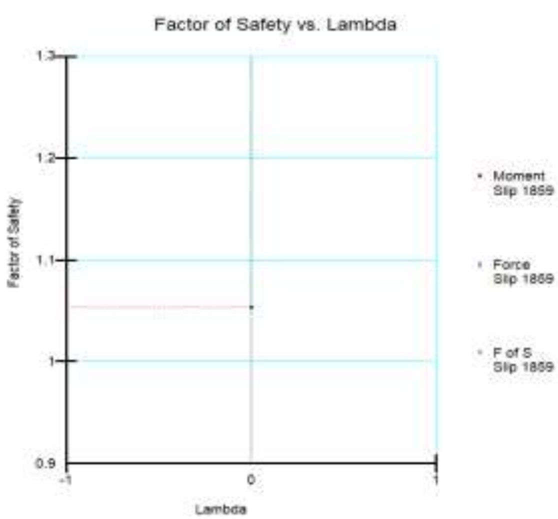
Factor of Safety vs. Lambda
1.3
1.2
1.1
1
0.9
Factor of Safety
-1
0
1
Lambda
Moment
Slip 1869
Force
Slip 1869
F of S
Slip 1869

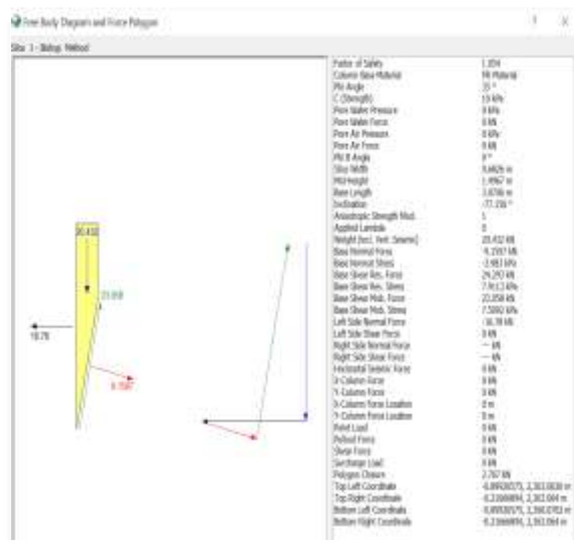

Using Janbu method

Case 1: When the Soil is fully saturated

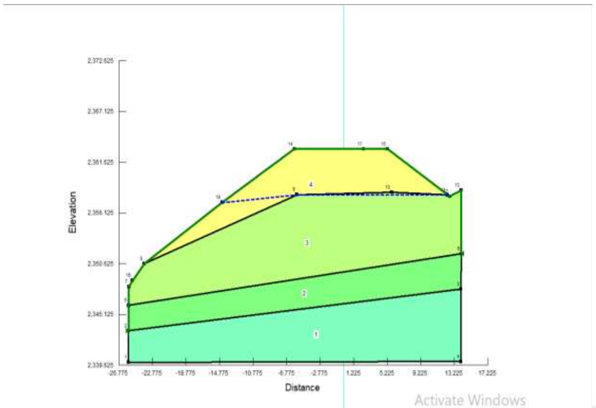

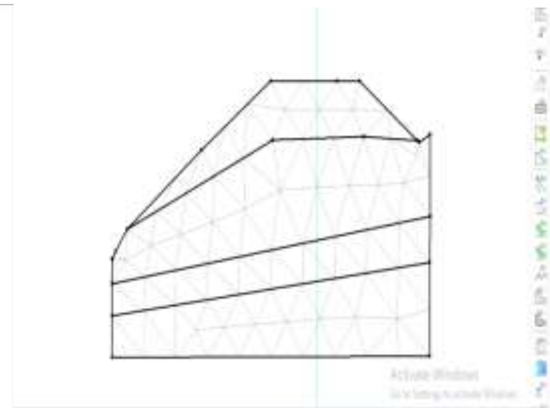

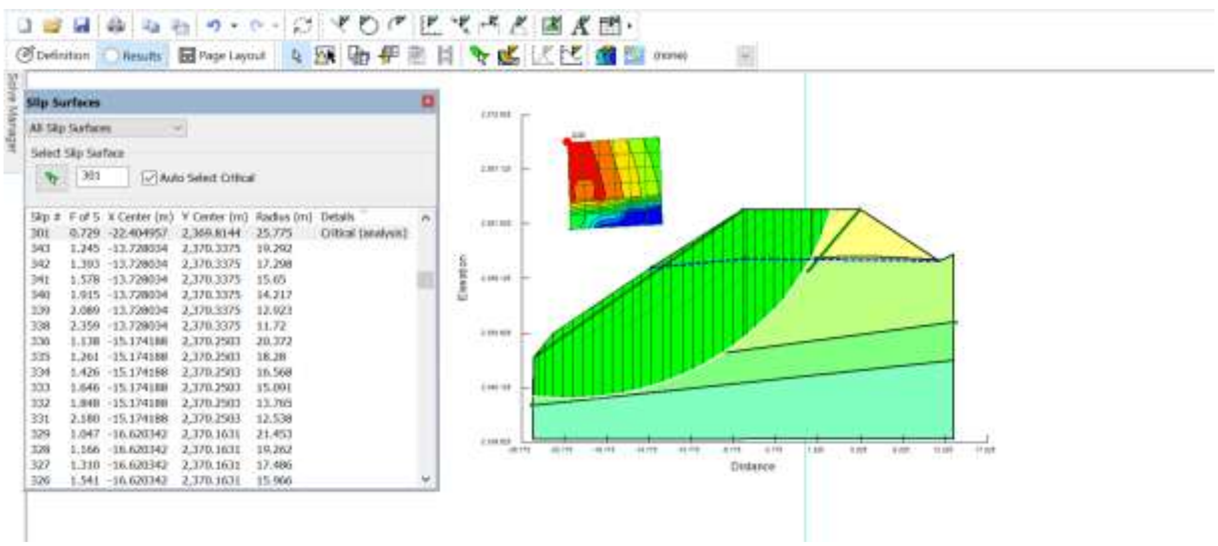

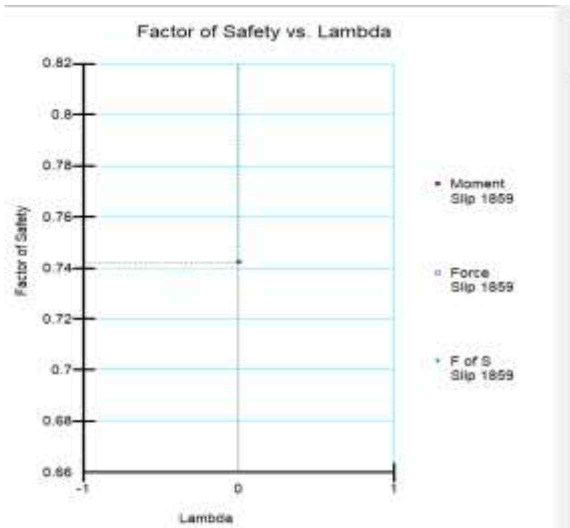

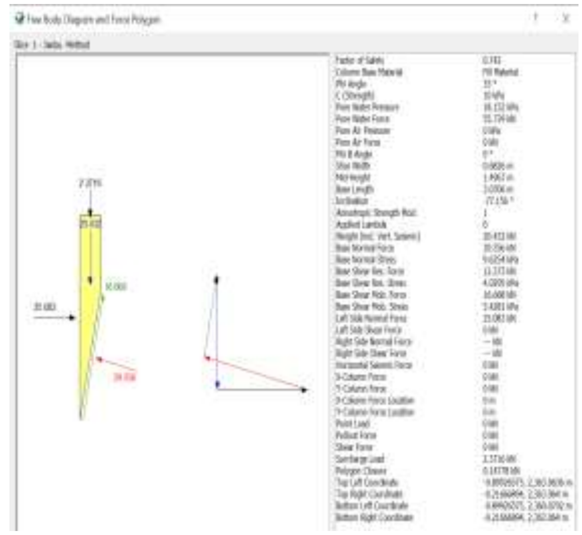

Case 2: When the Piezometric line is at the toe of the Embankment

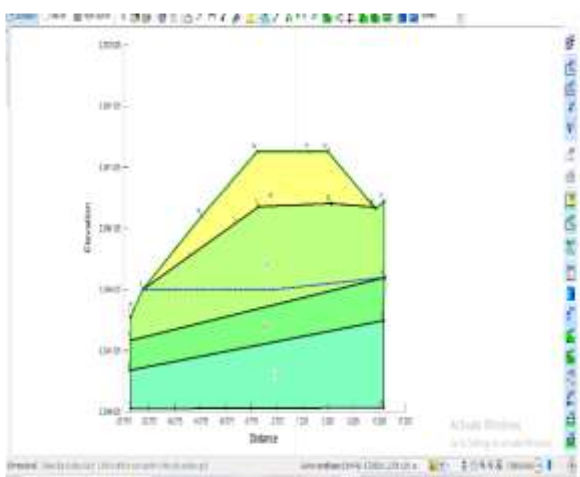

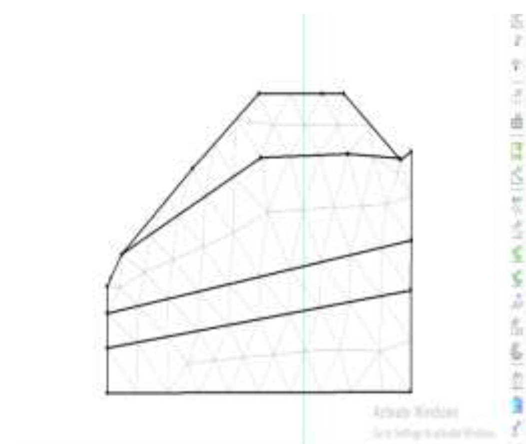

Slip Surfaces

All Slip Surfaces

Select Slip Surface

153 ☑ Auto Select Critical

Slip #	F of S	X Center (m)	Y Center (m)	Radius (m)	Details
153	0.755	-22.281880	2,365.4452	21.539	Critical (analysis)
343	1.272	-13.728034	2,370.3375	20.15	
342	1.403	-13.728034	2,370.3375	17.911	
341	1.588	-13.728034	2,370.3375	16.011	
340	2.019	-13.728034	2,370.3375	14.427	
339	2.082	-13.728034	2,370.3375	13.051	
338	2.315	-13.728034	2,370.3375	11.809	
336	1.155	-15.174188	2,370.2503	21.397	
335	1.277	-15.174188	2,370.2503	18.987	
334	1.428	-15.174188	2,370.2503	16.979	
333	1.676	-15.174188	2,370.2503	15.327	
332	1.918	-15.174188	2,370.2503	13.903	
331	2.139	-15.174188	2,370.2503	12.626	
329	1.040	-16.620342	2,370.1631	22.643	
328	1.180	-16.620342	2,370.1631	20.062	
327	1.317	-16.620342	2,370.1631	17.948	
326	1.522	-16.620342	2,370.1631	16.226